

I give permission for public access to my thesis and for copying to be done at the discretion of the archives' librarian and/or the College library.

Nicole Sonnert

Signature

5/1/2014

Date

**Population Dynamics and Size-Scaling Interactions of
Carcinus maenas and *Littorina obtusata* in Northern Maine**

by

Nicole D. Sonnert

A Paper Presented to the

Faculty of Mount Holyoke College in

Partial Fulfillment of the Requirements for

the Degree of Bachelors of Arts with

Honor

Department of Mathematics and Statistics and Department of Biological Sciences

South Hadley, MA 01075

May 2014

This paper was prepared
under the direction of
Professors L. David Smith (Smith), Christophe Golé (Smith) and Dylan Shepardson
for eight credits.

~For my family~

ACKNOWLEDGMENTS

I would like to thank my advisors L. David Smith, Chris Golé, and Dylan Shepardson. They have all been extremely supportive in my thesis endeavors over the past ten months. I am grateful for their valuable insights and contributions, as well as the large time investment they made in my project. I could not have done it without them. Margaret Robinson and Martha Hoopes have my gratitude for their time and expertise, as additional readers on my thesis committee.

My thanks also go to Elizabeth Sumner, Jessica Hopson, Yidan Jin, and Yu Jin for their help, companionship, and teamwork over the summer as well as throughout the year. In particular, I would like to recognize Yu Jin and Elizabeth Sumner for their collaboration on the Predator-Prey model. In addition, I gratefully acknowledge Sue Froehlich for her assistance with the Instron machine.

Finally, I would like to thank my mom, dad, and sister, who kept me grounded during this long journey.

Thank you all.

TABLE OF CONTENTS

List of Figures	vii
List of Tables	xi
Abstract	xiii
Chapter 1. Introduction	1
A. Bioinvasions and Invasive Predators	1
B. Critical Size Relationships in Predator-Prey Dynamics	2
C. Biology of the System of Study	5
D. Goals	7
Chapter 2. Population Surveys and Field Growth Experiments	10
A. Population Surveys: population abundances and size frequency distributions	10
B. Field Growth: <i>Littorina obtusata</i> growth rates in natural environment	18
C. Water Temperature	27
Chapter 3. Laboratory Critical Size of Vulnerability Experiments	30
A. Foraging Experiments: critical size of vulnerability of <i>Littorina obtusata</i> to <i>Carcinus maenas</i> predation	30
B. Crushing Force: proxy for vulnerability	36
Chapter 4. Modeling	38
A. Lotka-Volterra Model: predator-prey population density behavior	38
B. Size Projections: predicted growth within size frequency distributions of <i>Littorina obtusata</i> populations	42
C. <i>Littorina obtusata</i> Vulnerability to <i>Carcinus maenas</i> Predation: population-level model	50
Chapter 5. Discussion	59
Appendix A	71
Appendix B	74
Works Cited	81

LIST OF FIGURES

Chapter 1.

Figure 1. Allometric scaling on a log-log plot. Slope = 1, isometry, no disproportionate advantage. Slope > 1, positive allometry, predator has a disproportionate advantage. Slope < 1, negative allometry, prey has a disproportionate advantage.

Chapter 2.

Figure 2. (A-D) Size frequency distributions of male *Carcinus maenas* at Carrying Place Cove and Haycock Harbor in June and July. A) Carrying Place Cove, June. B) Carrying Place Cove, July. C) Haycock Harbor, June. D) Carrying Place Cove, July.

Figure 3. (A-D) Size frequency distributions of all *Carcinus maenas* at Carrying Place Cove and Haycock Harbor in June and July. A) Carrying Place Cove, June. B) Carrying Place Cove, July. C) Haycock Harbor, June. D) Haycock Harbor, July.

Figure 4. (A-D) Size frequency distributions of all *Littorina obtusata* at Carrying Place Cove and Haycock Harbor in June and July. A) Carrying Place Cove, June. B) Carrying Place Cove, July. C) Haycock Harbor, June. D) Haycock Harbor, July.

Figure 5. Initial shell height adjusted for a common initial shell length for Carrying Place Cove (CPC) and Haycock Harbor (HH) *Littorina obtusata* used in the field growth experiment.

Figure 6. Initial lip thickness adjusted for a common initial shell length for Carrying Place Cove (CPC) and Haycock Harbor (HH) *Littorina obtusata* used in the field growth experiment.

Figure 7. Final shell height adjusted for a common initial shell height for Carrying Place Cove (CPC) and Haycock Harbor (HH) *Littorina obtusata* used in the field growth experiment.

Figure 8. Final shell height adjusted for a common final shell length for Carrying Place Cove (CPC) and Haycock Harbor (HH) *Littorina obtusata* used in the field growth experiment.

Figure 9. Change in shell height adjusted for a common initial shell height for Carrying Place Cove (CPC) and Haycock Harbor (HH) *Littorina obtusata* used in the field growth experiment.

Figure 10. Final shell length adjusted for a common initial shell length for Carrying Place Cove (CPC) and Haycock Harbor (HH) *Littorina obtusata* used in the field growth experiment.

Figure 11. Final lip thickness adjusted for a common initial shell length for Carrying Place Cove (CPC) and Haycock Harbor (HH) *Littorina obtusata* used in the field growth experiment.

Figure 12. Final lip thickness adjusted for a common final shell length for Carrying Place Cove (CPC) and Haycock Harbor (HH) *Littorina obtusata* used in the field growth experiment.

Figure 13. Body weight adjusted for a common final shell length for Carrying Place Cove (CPC) and Haycock Harbor (HH) *Littorina obtusata* used in the field growth experiment.

Figure 14. Shell weight adjusted for a common final shell length for Carrying Place Cove (CPC) and Haycock Harbor (HH) *Littorina obtusata* used in the field growth experiment.

Figure 15. Body weight adjusted for a common shell weight for Carrying Place Cove (CPC) and Haycock Harbor (HH) *Littorina obtusata* used in the field growth experiment.

Figure 16. Average water temperature at high tide between June 10th and July 10th 2013 at Carrying Place Cove and Haycock Harbor in Lubec, ME.

Chapter 3.

Figure 17. Size scaling of *Carcinus maenas* and *Littorina obtusata* in June for four treatments.

Figure 18. Size scaling of *Carcinus maenas* and *Littorina obtusata* in July for four treatments.

Figure 19. Crushing force needed for Carrying Place Cove (CPC) and Haycock Harbor (HH) *Littorina obtusata* shells to break plotted against shell length.

Chapter 4.

Figure 20. *Littorina obtusata* projected density over time for Carrying Place Cove shown in blue and *Carcinus maenas* density over time for Carrying Place Cove shown in red. Month 0 corresponds to June 2013; month 4 corresponds to October 2013. Months 0 and 1 were measured.

Figure 21. *Littorina obtusata* projected density over time for Haycock Harbor shown in blue, and *Carcinus maenas* density over time for Haycock Harbor shown in red. Month 0 corresponds to June 2013; month 10 corresponds to April 2014. Months 0 and 1 were measured.

Figure 22. Comparison of *Littorina obtusata* frequencies from projections as well as actual June collected data at Carrying Place Cove in 2013.

Figure 23. Comparison of *Littorina obtusata* frequencies from projections as well as actual July collected data at Carrying Place Cove in 2013.

Figure 24. Comparison of *Littorina obtusata* frequencies from projections as well as actual June collected data at Carrying Place Cove in 2010.

Figure 25. Comparison of *Littorina obtusata* frequencies from projections as well as actual July collected data at Carrying Place Cove in 2010.

Figure 26. Comparison of *Littorina obtusata* frequencies from projections as well as actual August collected data at Carrying Place Cove in 2010.

Figure 27 A-D. Size frequency distribution of *Littorina obtusata* indicating relative degrees of vulnerability (dark solid=most vulnerable, light solid=moderately vulnerable, hatched=invulnerable—size refuge) in June and July at Carrying Place Cove and Haycock Harbor. A) Carrying Place Cove, June. B) Carrying Place Cove, July. C) Haycock Harbor, June. D) Haycock Harbor, July.

Appendix A.

Figure 28. Change in shell length adjusted for a common initial shell length for Carrying Place Cove (CPC) and Haycock Harbor (HH) *Littorina obtusata* used in the field growth experiment.

Figure 29. Change in lip thickness adjusted for a common initial shell length for Carrying Place Cove (CPC) and Haycock Harbor (HH) *Littorina obtusata* used in the field growth experiment.

Figure 30. Final lip thickness adjusted for a common initial lip thickness for Carrying Place Cove (CPC) and Haycock Harbor (HH) *Littorina obtusata* used in the field growth experiment.

Figure 31. Scaling of *Carcinus maenas* carapace width and claw height for Carrying Place and Haycock Harbor in June and July.

Figure 32. Comparison of *Littorina obtusata* frequencies from projections calculated based off of Carrying Place Cove growth rates as well as actual June collected data at Haycock Harbor in 2013.

Figure 33. Comparison of *Littorina obtusata* frequencies from projections calculated based off of Carrying Place Cove growth rates as well as actual July collected data at Haycock Harbor in 2013.

LIST OF TABLES

Chapter 2.

Table 1. Locations of study sites in Lubec, Maine.

Table 2. Kolmogorov-Smirnov goodness-of-fit tests for size frequency distributions of *Carcinus maenas* and *Littorina obtusata*.

Table 3. *Carcinus maenas* densities for Carrying Place Cove (CPC) and Haycock Harbor (HH) in June and July \pm one standard error. T-test results comparing densities between sites and months all had degrees of freedom of 4.

Table 4. *Littorina obtusata* densities for Carrying Place Cove (CPC) and Haycock Harbor (HH) in June and July \pm one standard error. T-test results comparing densities between sites and months all had degrees of freedom of 4.

Chapter 3.

Table 5. June scaling coefficients \pm one standard error for *Carcinus maenas* and *Littorina obtusata*.

Table 6. Analysis of covariance for feeding trials in June for all four combinations.

Table 7. July scaling coefficients \pm one standard error for *Carcinus maenas* and *Littorina obtusata*.

Table 8. Analysis of covariance for feeding trials in July for all four combinations.

Chapter 4.

Table 9. Parameter estimation using the least squares optimization for Carrying Place Cove and Haycock Harbor.

Table 10. Parameter sensitivity of parameters a , b , m_1 , m_2 , k using differentials and $t=0.000001$ for Carrying Place Cove and Haycock Harbor.

Table 11. Experimentally derived size scaling regression equations for *Carcinus maenas* and *Littorina obtusata* originating from the same site in June and July. The variable y represents \log_{10} [shell length] and x represents \log_{10} [carapace width].

Table 12. Absolute critical size of vulnerability of *Littorina obtusata* to *Carcinus maenas* on a population level as well as the percent of the *Littorina obtusata* population that is vulnerable to predation.

Table 13. Matrix of vulnerability to *Carcinus maenas* for *Littorina obtusata* at Carrying Place Cove in June 2013.

Table 14. Relative vulnerabilities for individual size classes of *Littorina obtusata* at Carrying Place Cove in June 2013.

Table 15. Matrix of vulnerability to *Carcinus maenas* for *Littorina obtusata* at Carrying Place Cove in July 2013.

Table 16. Relative vulnerabilities for individual size classes of *Littorina obtusata* at Carrying Place Cove in July 2013.

Table 17. Matrix of vulnerability to *Carcinus maenas* for *Littorina obtusata* at Haycock Harbor in June 2013.

Table 18. Relative vulnerabilities for individual size classes of *Littorina obtusata* at Haycock Harbor in June 2013.

Table 19. Matrix of vulnerability to *Carcinus maenas* for *Littorina obtusata* at Haycock Harbor in July 2013.

Table 20. Relative vulnerabilities for individual size classes of *Littorina obtusata* at Haycock Harbor in June 2013.

ABSTRACT

The European green crab, *Carcinus maenas*, invaded the mid-Atlantic coastline in the 1800s and has since expanded its range northwards into northern Maine and the Bay of Fundy (Scattergood 1952). *C. maenas* feeds on the native smooth periwinkle, *Littorina obtusata*. *C. maenas* and *L. obtusata* exhibit different growth strategies and absolute size of both species can affect the prey vulnerability. The critical size of vulnerability is the upper size at which a prey is vulnerable to a given predator size (Palmer 1990). The relationship of the critical size of *L. obtusata* vulnerability and *C. maenas* size indicates if there is isometric, positive-, or negative-allometric scaling between the two organisms (Palmer 1990).

In this project, spatial and temporal variation in the scaling relationship and critical size of vulnerability of *L. obtusata* fed to *C. maenas* was tested in a series of laboratory trials. Both species were collected from two coves (Carrying Place Cove and Haycock Harbor) in close proximity to each other and at two time points (June and July). *C. maenas* from both sites were fed *L. obtusata* from their home sites as well as from the other site. Offering *L. obtusata* to *C. maenas* from the opposite site allowed me to test if the scaling advantage relied on nuanced differences in the predator-prey interaction. It was found that in June, for 3 of 4 treatment combinations *L. obtusata* had an advantage over *C. maenas* as both increased in size. In July, the scaling relationship for *C. maenas* eating *L. obtusata* from the foreign site remained similar. Both of the scaling relationships for *C. maenas* eating *L. obtusata* from their home sites experienced a shift from allometry favoring *L. obtusata* towards isometry, and in the case of Haycock Harbor organisms, reaching allometry favoring *C. maenas*. The change in the scaling relationship for *C. maenas* and *L. obtusata* from the same site from June to July indicated a greater advantage for *C. maenas* in the second month than at the beginning. Based on size frequency distributions for *C. maenas*, populations at both sites contained more large individuals in July, suggesting *C. maenas* individuals molted and increased in size proportionately more than *L. obtusata* could, as they grow linearly. Moreover, the upper limit of the critical size of vulnerability for the largest *C. maenas* specimen found during the population survey, or more simply put as the size refuge threshold, increased at both sites from June to July, and the portion of the *L. obtusata* population that was vulnerable varied over space and time.

I found differences in size scaling interactions as well as in size frequency distributions and relative vulnerabilities over narrow temporal and spatial scales. The outcome of predator-prey interactions between *C. maenas* and *L. obtusata* in northern Maine relies on a subtle relationship between the two species.

CHAPTER 1. INTRODUCTION

A. Bioinvasions and Invasive Predators

As the global mobility of humans has dramatically increased in relatively recent times, they have knowingly and unknowingly transferred species around the world. Invasive species are often harmful to native organisms and cause shifts in the food web structure and a decrease in biodiversity (Vitousek et al. 1997). Studies about the dynamics of bioinvasions have the potential to provide insight into how future invasions could impact the invaded ecosystems and how humans might best respond to mitigate ecological damage.

Invasive predators can have multiple effects on the native species as well as on the dynamics of the ecosystem. They can alter nutrient availability by perturbing biogeochemical processes, trigger changes in biodiversity within food webs and communities, and physically modify the environment (Davis 2009). Invasive predators have been known to have a more detrimental effect on the native prey population than do native predators, resulting in smaller prey population sizes (Salo et al. 2007). For instance, seabird populations have often decreased, sometimes even to extinction, when invasive predators were introduced to the islands they use as their nesting grounds (Davis 2009). Moreover, invasive predators sometimes induce a change on an organismal level in the native prey phenotype (Smith 2009). One example of a phenotypic shift in a native prey is the change in body shape from a pelagic body type to a benthic

body type of yellow perch, when large predatory fish were introduced, in order to reduce predation or optimize benthic foraging (Lippert et al. 2007).

B. Critical Size Relationships in Predator-Prey Dynamics

The act of predation can be broken down into the following steps: detecting the prey, pursuing the prey, capturing, handling, and consuming the prey (Emerson et al. 1994). In a predator-prey interaction, the predator's goal is to optimize energy gain, while the prey's objective is to avoid being consumed. To optimize energy, the predator wants to efficiently eat prey that can be obtained relatively easily without physically harming itself and that has the most nutritional value. The prey can achieve its goal by either evading the initiation of the predation sequence or ending the interaction before consumption. Prey species have different avoidance tactics that are effective at different steps of predation; some prey move quickly as a strategy for avoiding initiation of predation, whereas others have physical defenses, such as toxins or armor, to avoid consumption.

The theory of optimal foraging, first developed by MacArthur and Pianka (1966), takes some of these steps into account and models the total energy benefit a predator obtains from its prey. An equation to model energy intake for a predator feeding on one prey species over time is $\frac{E}{T} = \frac{N_{e1}E_1 - C_s}{1 + N_{e1}H_1}$, where E is energy, T is time, N_{e1} is the number of prey, C_s is the search cost, and H_1 is the handling time (Werner and Mittelbach 1981). If a predator feeds on multiple prey species, the terms containing N_e would be added together. If the prey is harder to find and

capture, the predator must increase its search time and therefore decrease its energy benefit. If the prey is harder to handle and the edible portion of the organism is harder to obtain, the energy benefit that the predator receives decreases.

Physical limitations also play into the size aspect of predator-prey dynamics. This is particularly true for gape-limited predators as well as other predators who are constrained by other morphological limitations (Paine 1976; Forsman 1996). If the predator cannot consume the prey because the prey is too large, the prey has a size refuge. Emerson et al. (1994) noted that maximum prey body size scales with predator body size. For a given predator size, there is a critical size of vulnerability threshold for the prey. Above this threshold size, the predator is unable to successfully consume the prey; and below this size, the prey is vulnerable to predation (Paine 1976).

The scaling relationship between two organisms that are related by a predator-prey interaction can be described by the power function $Y=aM^b$, where Y and M are measures of prey and predator body size respectively, b is a scaling factor and a is a constant (Emerson et al. 1994). The Y generated by this equation is the critical size of vulnerability. Information about the size-scaling relationship can be more easily obtained by executing a logarithmic transformation, so that the linear relationship, $\log Y=\log a +b \log M$, results. The scaling factor, b , indicates how the two combatants, the predator and the prey, are scaling and which one has a disproportionate advantage, if there is one (Emerson et al. 1994). If $b=1$, the

relationship is isometric, meaning that neither party gains an advantage as each increases in size. If $b < 1$, there is a negative allometric relationship, indicating more effective prey defenses and thus increased handling time or greater risk of injury for the predator. In the predator-prey ‘arms race’, the prey would have the advantage and thus be “winning.” If $b > 1$, there is a positive allometric relationship, indicating a disproportionate advantage for the predator because an increase in predator body size is associated with a larger increase in the size of prey that it can consume (Emerson et al. 1994). This relationship can be easily visualized when plotted on a log-log plot, where $\log Y$ is on the vertical axis and $\log M$ is plotted on the horizontal axis (Figure 1).

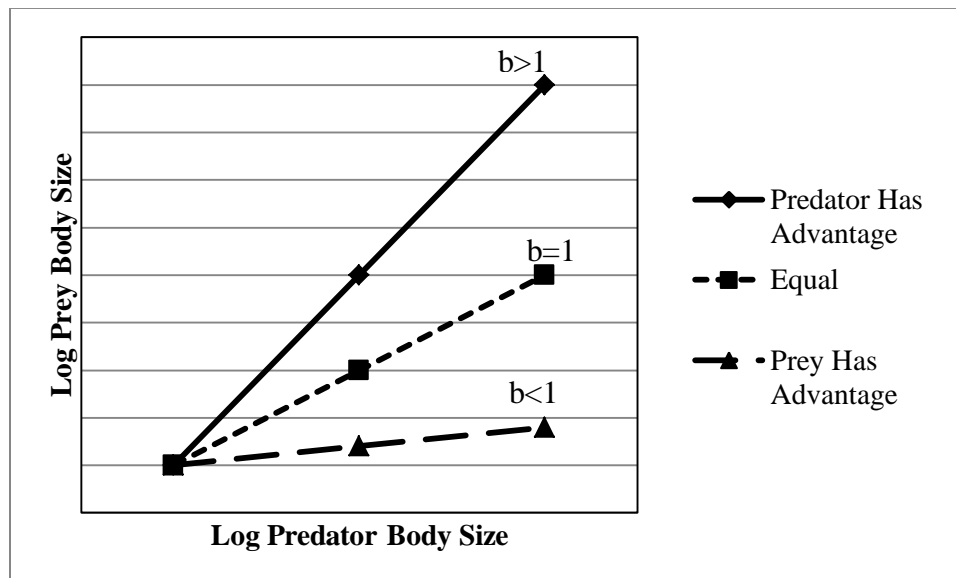


Figure 1. Allometric scaling on a log-log plot. Slope = 1, isometry, no disproportionate advantage. Slope > 1 , positive allometry, predator has a disproportionate advantage. Slope < 1 , negative allometry, prey has a disproportionate advantage.

C. Biology of the System of Study

Carcinus maenas, the European green crab, and *Littorina obtusata*, the smooth periwinkle, were studied in northern Maine. They make a good study system for inquiries about size-scaling relationships of a predator and a prey, because physiological attributes of both species dictate the outcome of their predation interaction. *C. maenas* has dimorphic claws. It breaks the *L. obtusata* shell with the larger crusher claw to gain access to the nutritious soft tissue, and the size and shape of the crusher claw are important determinants of predation success. Conversely, *L. obtusata*'s shell thickness, shape and size are important in reducing its vulnerability to crushing predators.

C. maenas is a littoral crab with carapace width ranging from about 2 mm for the youngest ones to 70 mm for the mature individuals (Welch and Churchill 1983). Its native range spans from Norway to Mauritania (Compton et al. 2010). It can tolerate many days out of water, withstand starvation, and tolerate large temperature and salinity ranges, which contributes to successful invasions (Dow and Wallace 1952; Behrens Yamada 2001). It is a well-known invader and has established itself in habitats around the world, such as off the coast of Australia (Ahyong 2005), South Africa, Japan, and the western United States (Carlton and Cohen 2003). The earliest known invasive presence of *C. maenas* is in the 1800s in the mid-Atlantic region of the United States (Say 1817; Scattergood 1952). The *C. maenas* population then moved northward extending to Cape Cod in Massachusetts by the 1870s and to southern Maine by the 1890s (Carlton and

Cohen 2003). Eventually, in 1952, the *C. maenas* population reached Lubec, Maine (Scattergood 1952). Since then, *C. maenas* has moved further north and has populated the Bay of Fundy. Lower *C. maenas* population densities as well as more ephemeral populations are observed in the northern Gulf of Maine (Seeley 1986). This is most likely due to colder water temperatures in the northern Gulf of Maine and the Bay of Fundy compared to surrounding waters. As water temperatures have risen over the past century, *C. maenas* has been able to extend its range further north (Carson and Hubbell 1998).

C. maenas molt at discrete time points and can increase up to 30% in size (Behrens Yamada 2001). Both water temperature and food affect how often *C. maenas* molts and by how much they increase in size. They only molt when it is warm enough, and in the winter, when the water temperature drops below 10°C, *C. maenas* stop molting and retreat into hiding spots (Behrens Yamada 2001). *C. maenas* with low food availability do not increase as much in size per molt (Behrens Yamada 2001).

C. maenas feeds on a wide variety of organisms from at least 158 genera, including mollusks and gastropods (Cohen et al. 1995). When given a choice of several common hard-shelled prey, however, *C. maenas* preyed on *L. obtusata* preferentially (Rangely and Thomas 1987).

L. obtusata is found natively throughout coasts in the North Atlantic Ocean ranging from Europe to the northern parts of the United States as well as Canada (Reid 1996). *L. obtusata* is found in the mid-littoral zone on sheltered shores

where brown macroalgae, such as *Ascophyllum nodosum*, are found (Trussell 1997; Reid 1996). *L. obtusata* has a slightly different morphology based on its environment: more northern specimens are found to have larger shells; *L. obtusata* found closer to exposed shores (they are never found in truly exposed sites) exhibit smaller shells and lower spires (Reid 1996). The global maximum size of *L. obtusata* is about 18 mm when found in a moderate ecotype (Reid 1996).

L. obtusata hatchlings mainly appear in May and June but continue to appear in lesser amounts until about October (Goodwin 1977). *L. obtusata* populations are generally bimodal with distinct adult and juvenile peaks, where the shell lengths of the adult peak remain about constant and the shell lengths of the juvenile peak increase over a year, taking about 18 months to reach maturity and enter the largest size class (Goodwin 1977). They continuously grow and lay down calcium carbonate at the leading edge of the shell and, in northern Maine, reach a maximum size of about 15 mm. Once they get to this size, they continue to thicken their shell (Kennedy 2009). *L. obtusata*, like most snails, exhibit shell growth rates that change over time in a logistic fashion (Nishida and Napompeth 1975).

D. Goals

In this study, the size-scaling relationship between *Carcinus maenas* and *Littorina obtusata*, an invasive predator and a native prey, and their population

dynamics in relation to their size frequency distributions were investigated on a local scale in northern Maine over a narrow time scale.

QUESTIONS:

1. Are there similar densities and size frequency distributions of *C. maenas* and *L. obtusata* over narrow spatial and temporal scales?
2. Does *C. maenas* or *L. obtusata* gain a disproportionate advantage over the other as each increases in size?
3. Does the size-scaling relationship between *C. maenas* and *L. obtusata* differ over narrow spatial or temporal scales?
4. Does the size-scaling relationship depend on nuanced differences between organisms (i.e., the nuanced differences could relate to shell resistance to crushing, growth rates, shell thickness, shell shape, familiarity in handling, etc.)?
5. How do the *C. maenas* and *L. obtusata* populations interact over time, and are the dynamical behaviors of the population densities different over a narrow spatial scale?
6. What portion of the *L. obtusata* population is vulnerable to *C. maenas* predation, to what degree are *L. obtusata* vulnerable, and is this evident in the *L. obtusata* size frequency distributions?

A series of field and laboratory experiments were conducted and mathematical models were created in attempts to answer these questions and elucidate the

subtleties, if present, of the size-scaling relationship and population dynamics of *C. maenas* and *L. obtusata*.

CHAPTER 2. POPULATION SURVEYS AND FIELD GROWTH EXPERIMENTS

Data were collected from two study sites, Carrying Place Cove and Haycock Harbor, in Lubec, Maine (Table 1). Both were similar in furoid cover, boulder size and distribution as well as in the level of wave exposure. Data were collected from 10-13 June 2013 and again from 9-10 July 2013.

Table 1. Locations of study sites in Lubec, Maine.

Site	Coordinates
Carrying Place Cove	44°48'25"N 66°58'51"W
Haycock Harbor	44°45'12"N 67°03'47"W

A. Population Surveys: population abundances and size frequency distributions

a. Materials and Methods

Carcinus maenas and *Littorina obtusata* were collected from Carrying Place Cove and Haycock Harbor in Lubec, Maine, once at each site during the June 2013 and during the July 2013 collections at morning and evening low tides.

1. *C. maenas*: Individuals were collected by overturning rocks along three transects at each site (high, middle, low) for 10 minutes per transect. The same person conducted all of the time searches at each transect, site, and on each month, for consistency. The specimens were sexed and carapace width, crusher claw height, depth and length, as well as the cutter claw height were

measured using digital calipers to (± 0.01 mm). Individuals with carapace widths less than 10.0 mm were excluded from size frequency distributions and densities because it was hard to make sure every small *C. maenas* encountered was accounted for.

2. *L. obtusata*: A 10 m tape was laid out in the middle section of the intertidal parallel to the water. A random number generator was used to pick three numbers, which corresponded to meter marks along the transect. The middle of the top edge of a 0.25 m x 0.25 m quadrat was placed at the randomly picked meter mark. All *L. obtusata* in the marked off area were collected, making sure the organisms on the rocks and the *Ascophyllum* were taken. This was executed three times. Shell length, shell height, and lip thickness were measured with digital calipers to (± 0.01 mm).

To compare the amount of *C. maenas* and *L. obtusata* present at each site, population densities were calculated by converting the frequencies of *C. maenas* determined during the time searches to units of crabs/minute, and *L. obtusata* frequencies from the quadrats, to units of snails/m² for each of the three time searches or quadrat replications. T-tests in Excel were executed with an alpha value of 0.05 to determine if the densities at different sites and different months varied significantly.

Kolmogorov-Smirnov tests were completed, using the JMP 10 statistical software package, to test the difference of size frequency distributions between

the two collection times and between the sites. Size was measured as carapace width for *C. maenas* and as shell length for *L. obtusata*.

b. Results

Carcinus maenas. At both Carrying Place Cove and Haycock Harbor, the size frequency distributions differed significantly between the two months for both the entire population, as well as for just the male *C. maenas* (Table 2). At both sites, the size frequency distributions shifted towards the larger range between months (Figure 2 A-D; Figure 3 A-D). In June, there was a significant difference between the size frequency distributions between the two sites for the whole populations as well as for male *C. maenas* (Table 2). The *C. maenas* at Haycock Harbor were found not only in a narrower size distribution, but also the overall size of the Haycock Harbor *C. maenas* was much smaller than that of *C. maenas* found at Carrying Place Cove in June (Figure 2 A, C; Figure 3 A, C). In contrast, in July, no significant difference in size frequency distribution was found between Carrying Place Cove and Haycock Harbor for the total populations or for the male individuals (Table 2; Figure 2 B, D; Figure 3 B, D).

Littorina obtusata. There was no significant difference at Carrying Place Cove in the size frequency distributions for *L. obtusata* between June and July (Table 2). Both size frequency distributions were skewed towards the upper sizes (Figure 4 A, B). However, there was a significant difference at Haycock Harbor in the *L. obtusata* size frequency distributions between June and July (Table 2). There were more small and medium *L. obtusata* found in June at Haycock Harbor, and the

distribution looked more normal in July than in June (Figure 4 C, D). In June, there was a significant site difference in the size frequency distributions with Carrying Place Cove *L. obtusata* skewed towards the larger sizes. In July, this site difference abated, with the Haycock Harbor *L. obtusata* size frequency distribution skewed towards larger sizes (Table 2; Figure 4 A, C).

Table 2. Kolmogorov-Smirnov goodness-of-fit tests for size frequency distributions of *Carcinus maenas* and *Littorina obtusata*.

Species	Sampling Sites Compared	Sampling Dates Compared	KS	Site Freq. Dist. Differs (Y/N)	P
All <i>C. maenas</i>	Carrying Place Cove	June-July	0.13730	Y	0.0429*
All <i>C. maenas</i>	Haycock Harbor	June-July	0.28319	Y	<0.0001*
Male <i>C. maenas</i>	Carrying Place Cove	June-July	0.23405	Y	0.0020*
Male <i>C. maenas</i>	Haycock Harbor	June-July	0.36078	Y	<0.0001*
All <i>C. maenas</i>	Carrying Place Cove-Haycock Harbor	June	0.21163	Y	0.0008*
All <i>C. maenas</i>	Carrying Place Cove-Haycock Harbor	July	0.07642	N	0.6034
Male <i>C. maenas</i>	Carrying Place Cove-Haycock Harbor	June	0.21328	Y	0.0071*
Male <i>C. maenas</i>	Carrying Place Cove-Haycock Harbor	July	0.08621	N	0.7818
<i>L. obtusata</i>	Carrying Place Cove	June-July	0.10847	N	0.2517
<i>L. obtusata</i>	Haycock Harbor	June-July	0.28061	Y	0.0111*
<i>L. obtusata</i>	Carrying Place Cove-Haycock Harbor	June	0.33640	Y	<0.0001*
<i>L. obtusata</i>	Carrying Place Cove-Haycock Harbor	July	0.17343	N	0.0575

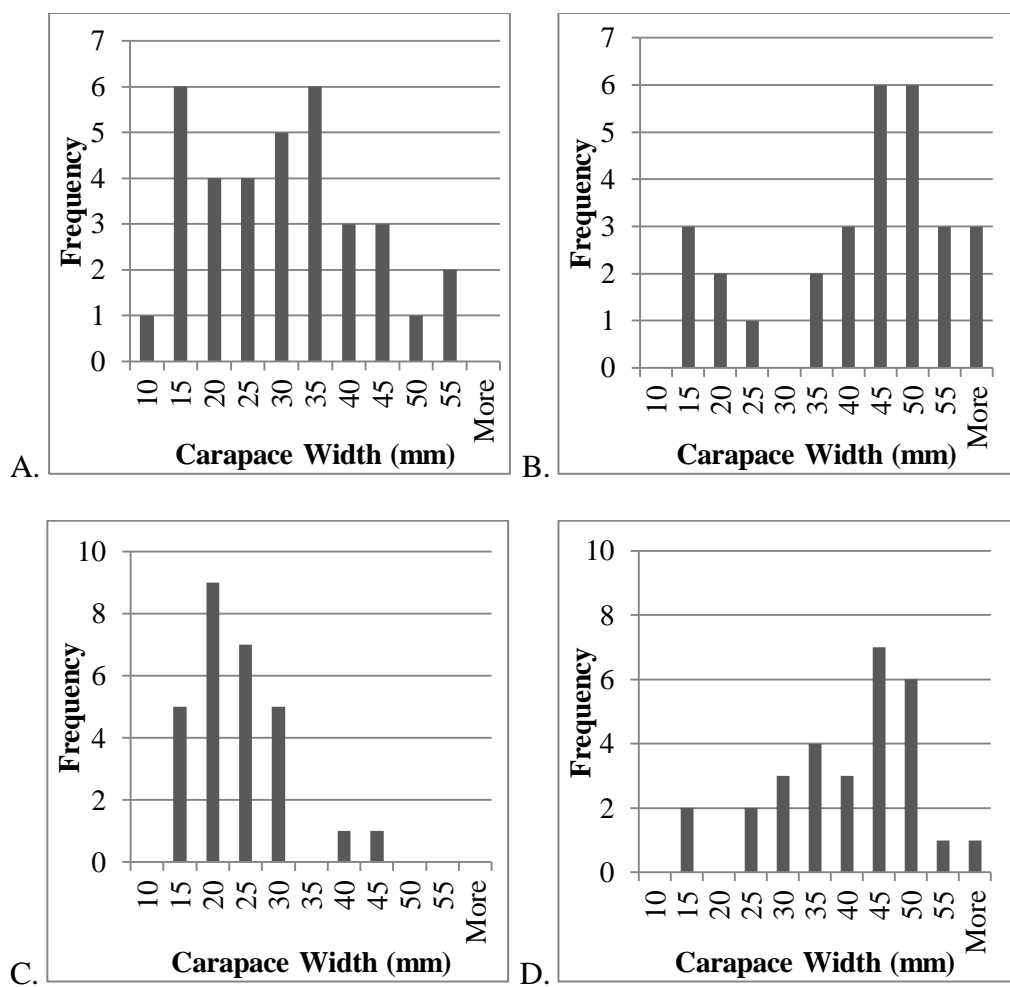


Figure 2. (A-D) Size frequency distributions of male *Carcinus maenas* at Carrying Place Cove and Haycock Harbor in June and July. A) Carrying Place Cove, June. B) Carrying Place Cove, July. C) Haycock Harbor, June. D) Haycock Harbor, July.

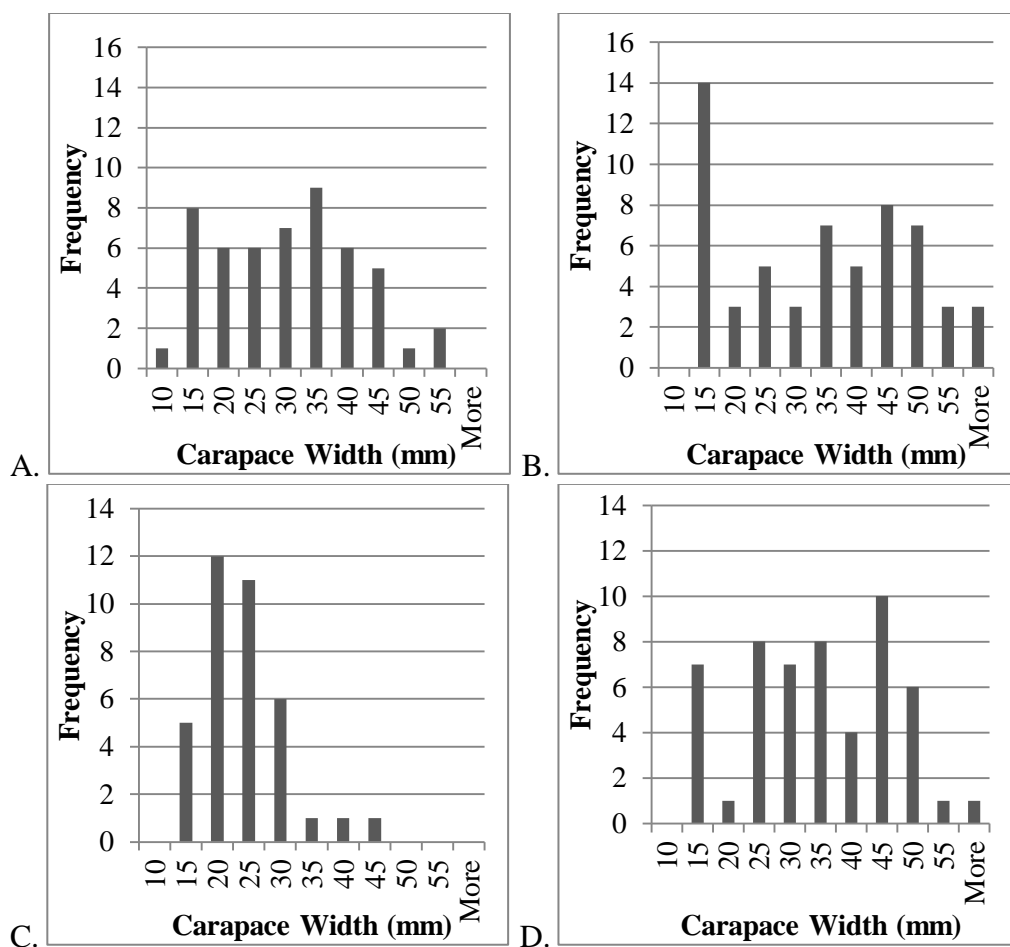


Figure 3. (A-D) Size frequency distributions of all *Carcinus maenas* at Carrying Place Cove and Haycock Harbor in June and July. A) Carrying Place Cove, June. B) Carrying Place Cove, July. C) Haycock Harbor, June. D) Haycock Harbor, July.

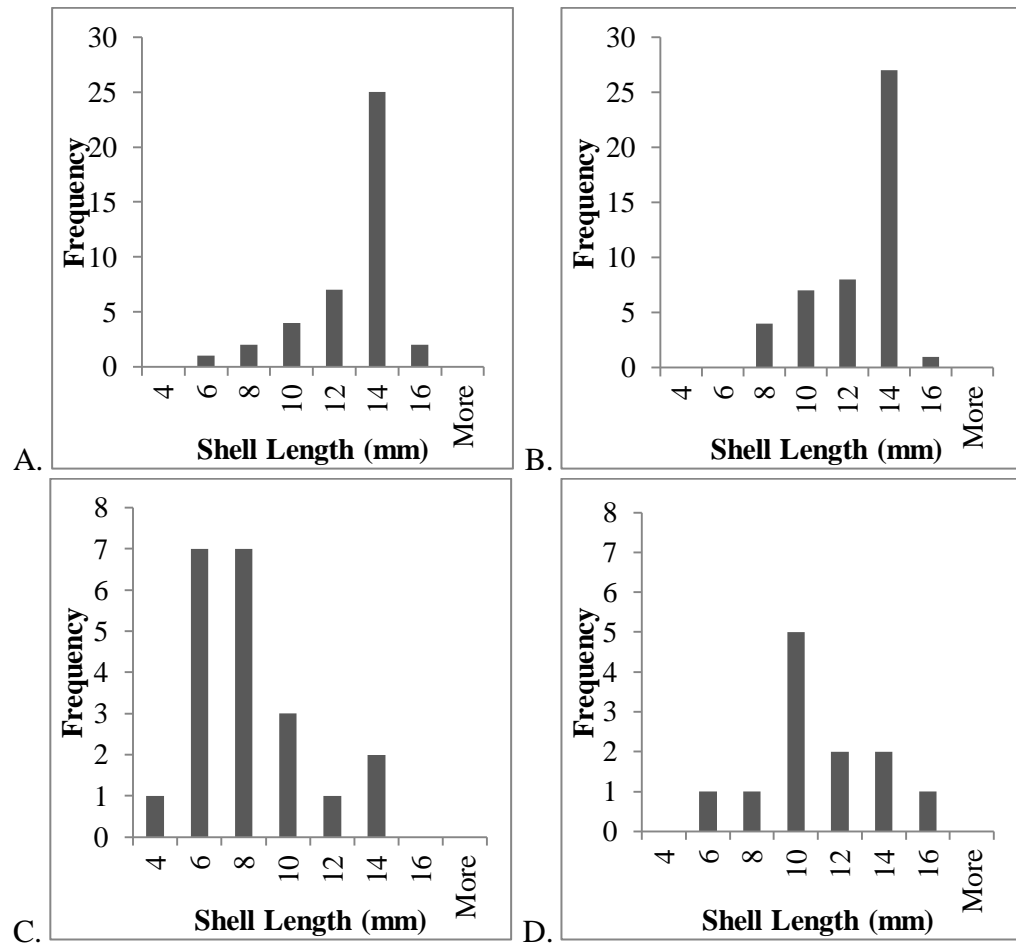


Figure 4. (A-D) Size frequency distributions of all *Littorina obtusata* at Carrying Place Cove and Haycock Harbor in June and July. A) Carrying Place Cove, June. B) Carrying Place Cove, July. C) Haycock Harbor, June. D) Carrying Place Cove, July.

At Carrying Place Cove, there were higher densities of both *C. maenas* and *L. obtusata* in July than in June (Table 3; Table 4). At Haycock Harbor, there was a higher density of *C. maenas* found in July than in June, and lower densities of *L. obtusata* in July than in June (Table 3; Table 4). Although relative variations are apparent, there were no significant differences found between any *C. maenas* or *L. obtusata* comparison combination (Table 3; Table 4). As a remark on the

frequencies of the organisms during each replication, similar numbers of individuals were not found, thus limiting the effectiveness of a t-test.

Table 3. *Carcinus maenas* densities for Carrying Place Cove (CPC) and Haycock Harbor (HH) in June and July \pm one standard error. T-test results comparing densities between sites and months all had degrees of freedom of 4.

Month	CPC	HH	P-Value
June	218.67 \pm 61.51	112.00 \pm 79.64	0.2378
July	250.67 \pm 46.19	64.00 \pm 24.44	0.0886
P-Value	0.7664	0.4103	

Table 4. *Littorina obtusata* densities for Carrying Place Cove (CPC) and Haycock Harbor (HH) in June and July \pm one standard error. T-test results comparing densities between sites and months all had degrees of freedom of 4.

Month	CPC	HH	P-Value
June	1.70 \pm 0.26	1.93 \pm 0.22	0.2455
July	1.23 \pm 0.38	1.77 \pm 0.15	0.7002
P-Value	0.6383	0.1120	

B. Field Growth: *Littorina obtusata* growth rates in natural environment

a. Materials and Methods

To compare growth rates of *Littorina obtusata*, 25 *L. obtusata* specimens each were collected at Carrying Place Cove and Haycock Harbor on 10 and 11 June 2013, with an overall size range of 7.18 – 12.06 mm shell length. The individuals were marked with five distinguishable symbols using a paint pen and the marks were sealed with cyanoacrylate glue. Shell length and shell height were measured once, and the lip thickness was measured twice. All measurements were made using digital calipers to (\pm 0.01 mm). Growth containers consisted of round Tupperware containers with dimensions of a 10.5 cm diameter and a 7.5 cm height, modified with holes on the sides and tops covered with mesh for each site.

Five marked and measured *L. obtusata* were put in each container. There were a total of five containers for each site. The following morning, *Ascophyllum* was put into the small containers containing *L. obtusata* to eat. The small containers were placed into larger Tupperware containers that also had mesh windows and had dimensions of 22.0 cm in length and width and 12.0 cm in height. The larger plastic containers were secured to bricks and distributed about 10 meters apart along the intertidal. The containers were collected 29 days later. Four out of the five containers from Haycock Harbor and all five containers from Carrying Place Cove were recovered. The 20 *L. obtusata* from Haycock Harbor and the 25 *L. obtusata* from Carrying Place Cove were transported back to Northampton, Massachusetts in coolers. The *L. obtusata* were measured again to obtain final measurements in order to determine growth of *L. obtusata* at both sites.

After the field growth experiment concluded, the recovered *L. obtusata* from the field growth experiment (25 from Carrying Place Cove and 20 from Haycock Harbor) were frozen for destructive sampling to determine shell and body weights. Once frozen, the shell was separated from the soft tissue and both components were put in individual, pre-weighed plastic boats. The body and shell samples were dried in an oven for two days at 40°C and then were weighed using a digital balance.

Analysis of covariance (ANCOVA) tests were performed on log-transformed data in JMP 10 to determine if the growth was different between *L. obtusata* at Carrying Place Cove and Haycock Harbor. In executing the ANCOVA, the

containers and the sites were nested, as the individuals within the containers were not independent.

b. Results

At the outset of the field growth experiment, shell height, adjusted for a common shell length, was significantly greater for Carrying Place Cove *Littorina obtusata* than for Haycock Harbor *L. obtusata* ($p=0.0315$) (Figure 5). In June, Haycock Harbor *L. obtusata* had significantly thicker shell lips, adjusted for shell length, than Carrying Place Cove *L. obtusata* ($p=0.0081$) (Figure 6).

After 29 days, Carrying Place Cove *L. obtusata* had significantly larger final shell heights, adjusted for initial shell height (or shell length), than did Haycock Harbor *L. obtusata* ($p=0.0313$; $p=0.0029$, respectively) (Figure 7; Figure 8). This relationship did not hold up when testing the change in shell height for a common initial shell height ($p=0.3572$) (Figure 9).

Carrying Place Cove *L. obtusata* exhibited significantly larger final shell lengths for a common initial shell length than Haycock Harbor *L. obtusata*, indicated by a p value of 0.006 (Figure 10). This significant relationship also stood for a change in shell length for a common initial shell length ($p=0.0215$) (Appendix A, Figure 28).

At both sites, the *L. obtusata*'s lip thicknesses decreased, and the change in lip thickness for a common initial shell length, as well as the final lip thickness adjusted for a common initial lip thickness, were not significantly different ($p=0.1064$; $p=0.5511$, respectively) (Appendix A, Figure 29; Appendix A, Figure

30). Adjusted for a common initial shell length as well as for a common final shell length, Haycock Harbor *L. obtusata* had significantly larger final lip thicknesses than Carrying Place Cove individuals ($p=0.0237$; $p=0.0331$, respectively) (Figure 11; Figure 12).

For a common final shell length, the body weight of the *L. obtusata* at the different sites were not significantly different, although a trend suggested that Carrying Place Cove *L. obtusata* had a larger body mass compared to individuals from Haycock Harbor, indicated by a p-value of 0.0901 (Figure 13). Similarly, for a common final shell length, the final shell weight of *L. obtusata* at both sites was not significantly different, although a trend suggested that Haycock Harbor *L. obtusata* had heavier shells compared to *L. obtusata* from Carrying Place Cove ($p=0.0667$) (Figure 14).

For a common shell weight, there was a significant difference in body weight between the two sites. There was a larger body weight for Carrying Place Cove *L. obtusata* than for Haycock Harbor *L. obtusata* ($p=0.0185$) (Figure 15).

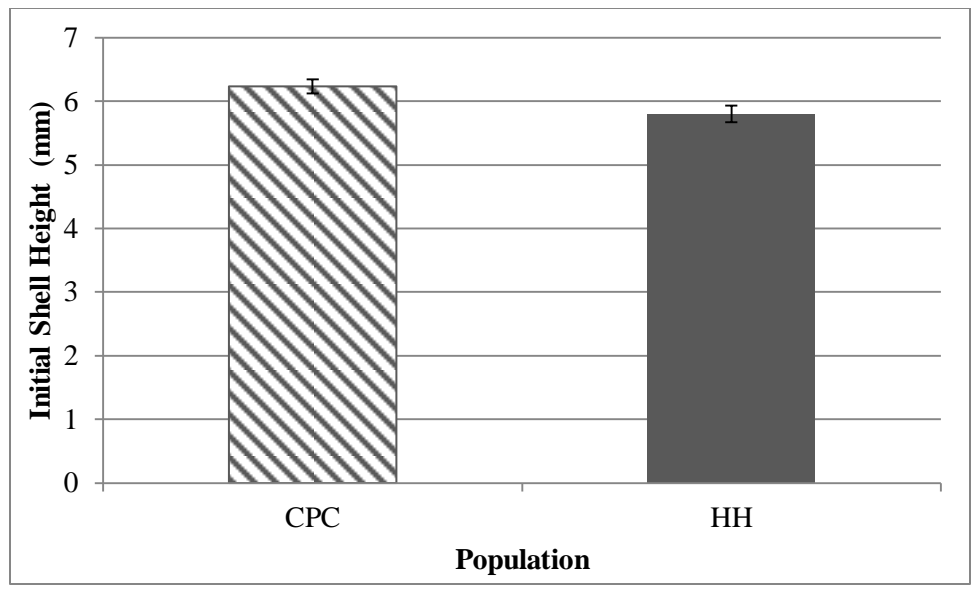


Figure 5. Initial shell height adjusted for a common initial shell length for Carrying Place Cove (CPC) and Haycock Harbor (HH) *Littorina obtusata* used in the field growth experiment.

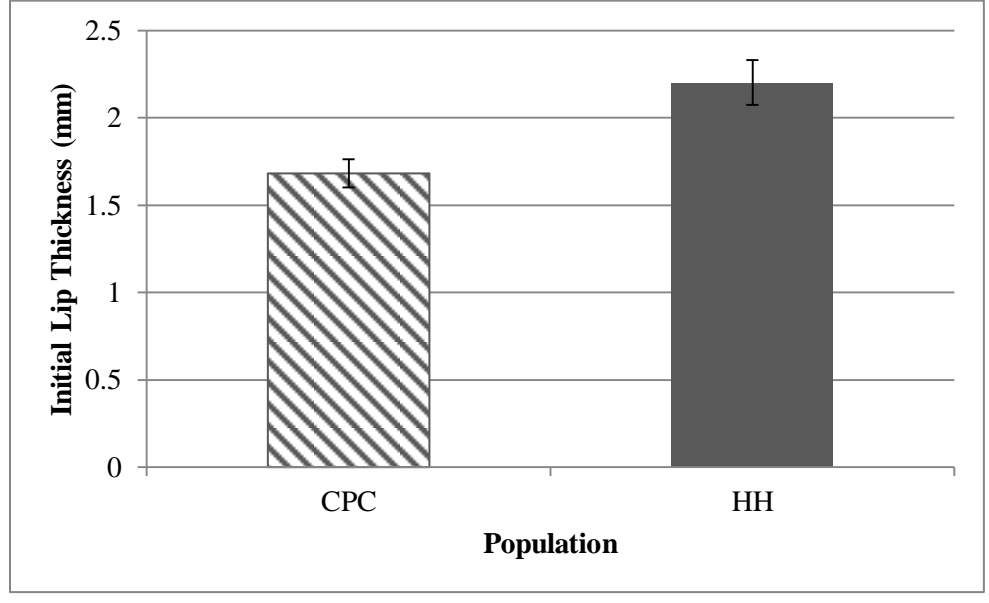


Figure 6. Initial lip thickness adjusted for a common initial shell length for Carrying Place Cove (CPC) and Haycock Harbor (HH) *Littorina obtusata* used in the field growth experiment.

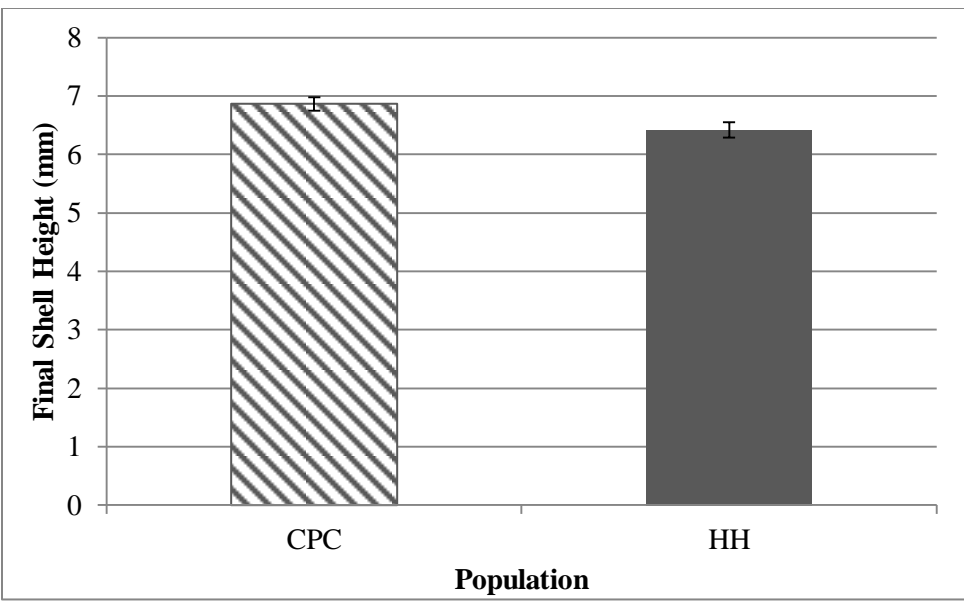


Figure 7. Final shell height adjusted for a common initial shell height for Carrying Place Cove (CPC) and Haycock Harbor (HH) *Littorina obtusata* used in the field growth experiment.

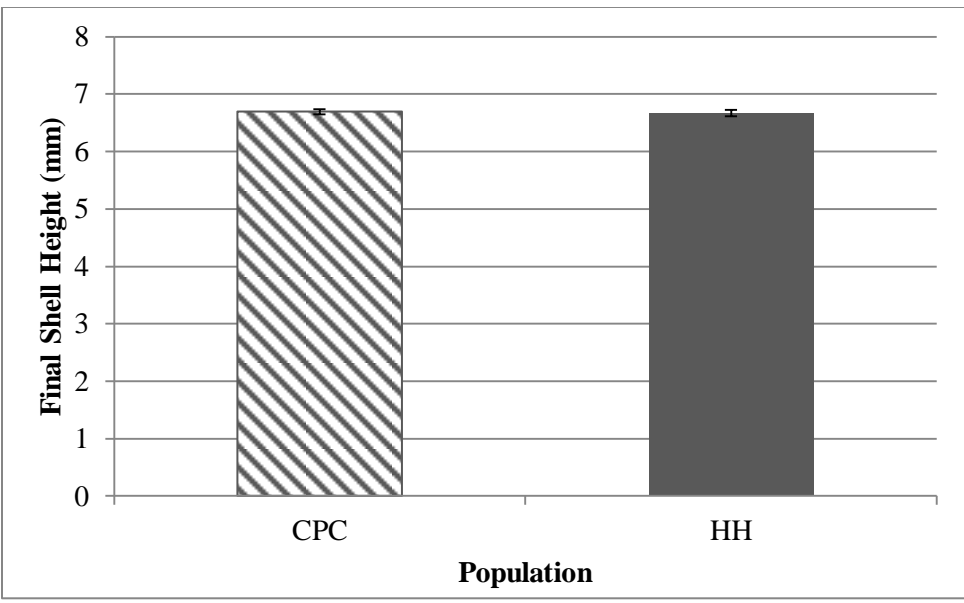


Figure 8. Final shell height adjusted for a common final shell length for Carrying Place Cove (CPC) and Haycock Harbor (HH) *Littorina obtusata* used in the field growth experiment.

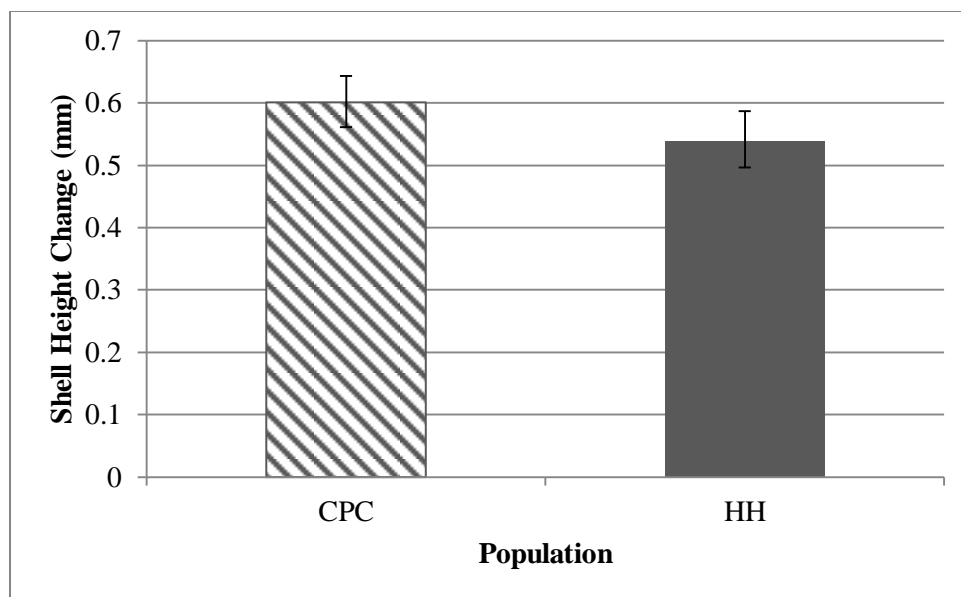


Figure 9. Change in shell height adjusted for a common initial shell height for Carrying Place Cove (CPC) and Haycock Harbor (HH) *Littorina obtusata* used in the field growth experiment.

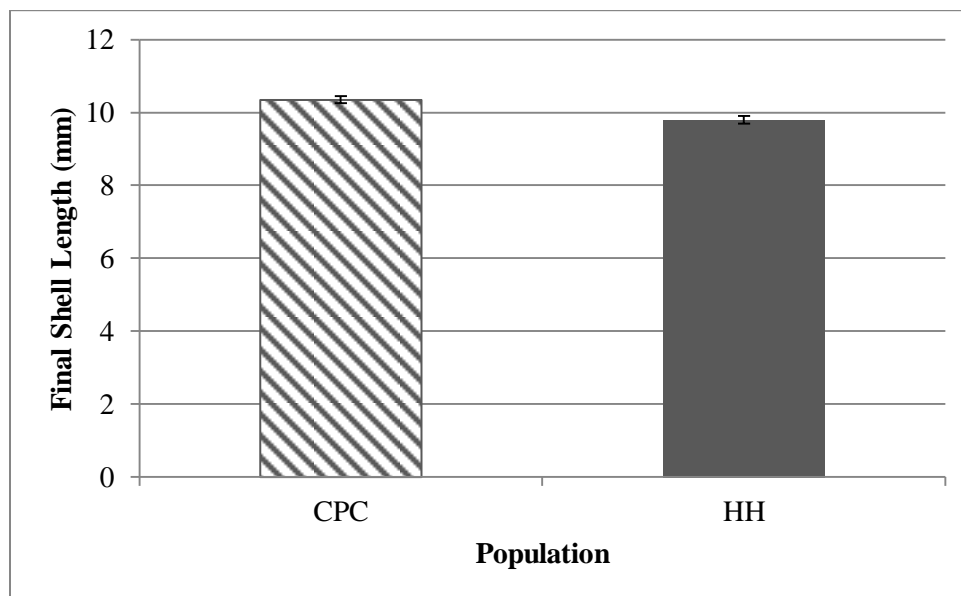


Figure 10. Final shell length adjusted for a common initial shell length for Carrying Place Cove (CPC) and Haycock Harbor (HH) *Littorina obtusata* used in the field growth experiment.

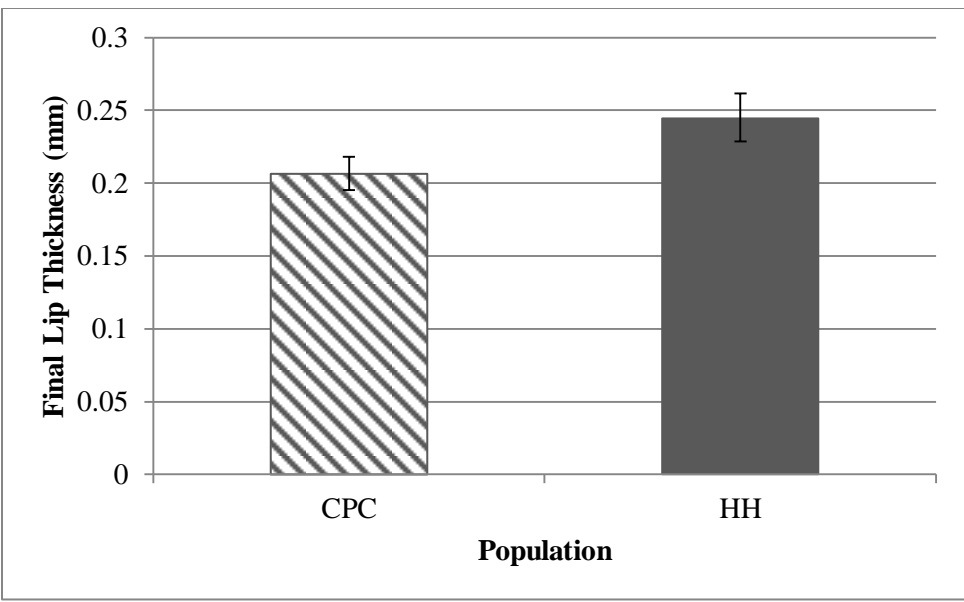


Figure 11. Final lip thickness adjusted for a common initial shell length for Carrying Place Cove (CPC) and Haycock Harbor (HH) *Littorina obtusata* used in the field growth experiment.

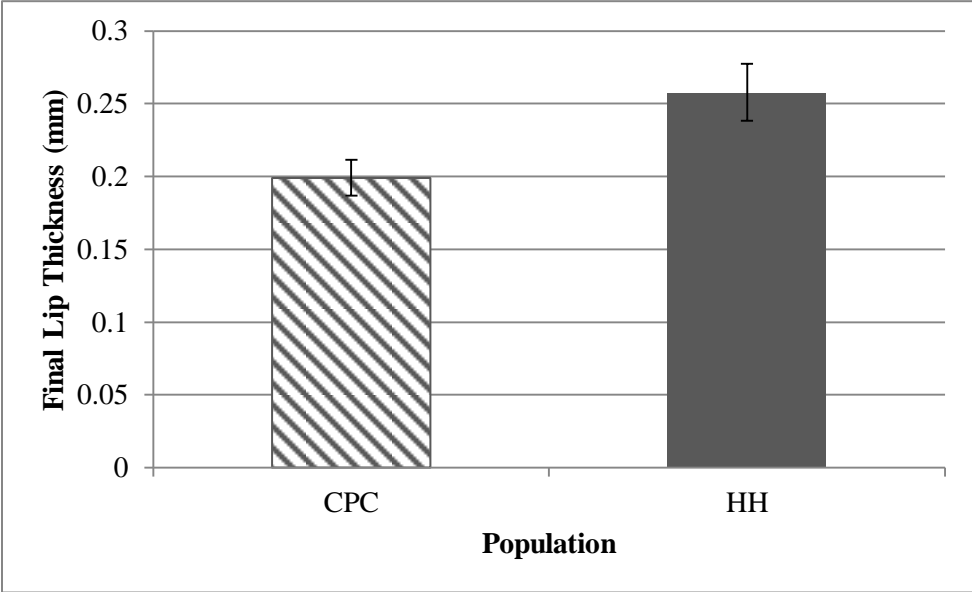


Figure 12. Final lip thickness adjusted for a common final shell length for Carrying Place Cove (CPC) and Haycock Harbor (HH) *Littorina obtusata* used in the field growth experiment.

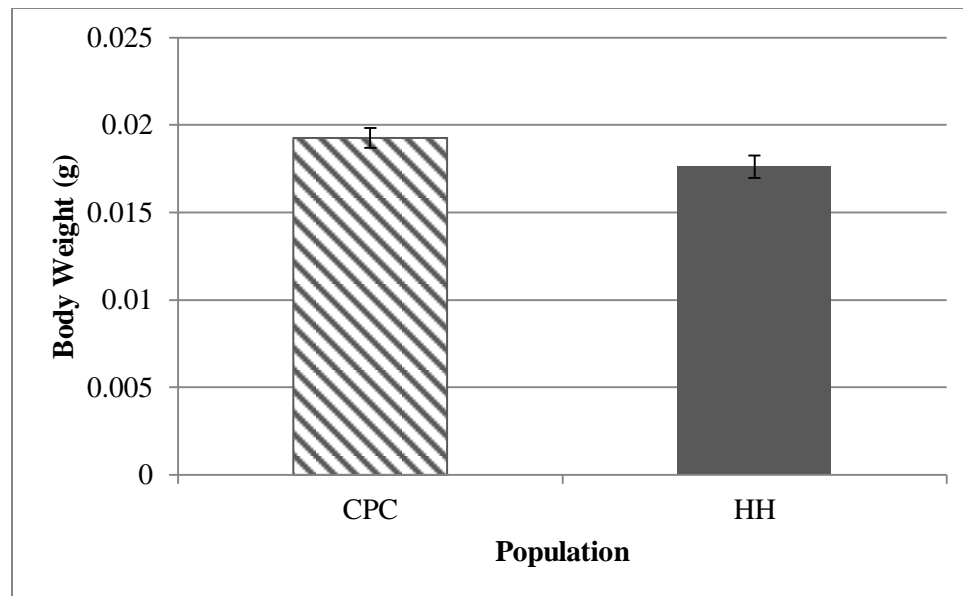


Figure 13. Body weight adjusted for a common final shell length for Carrying Place Cove (CPC) and Haycock Harbor (HH) *Littorina obtusata* used in the field growth experiment.

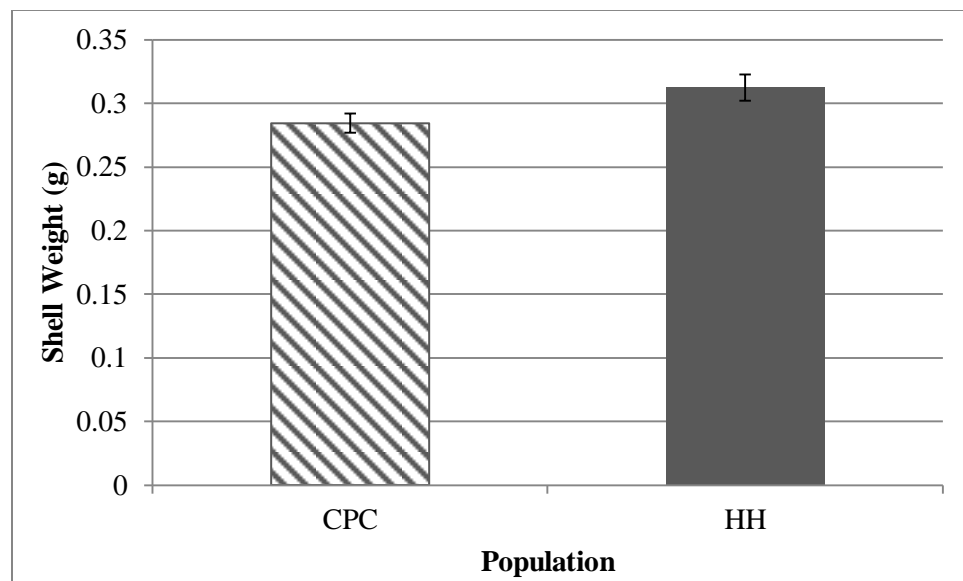


Figure 14. Shell weight adjusted for a common final shell length for Carrying Place Cove (CPC) and Haycock Harbor (HH) *Littorina obtusata* used in the field growth experiment.

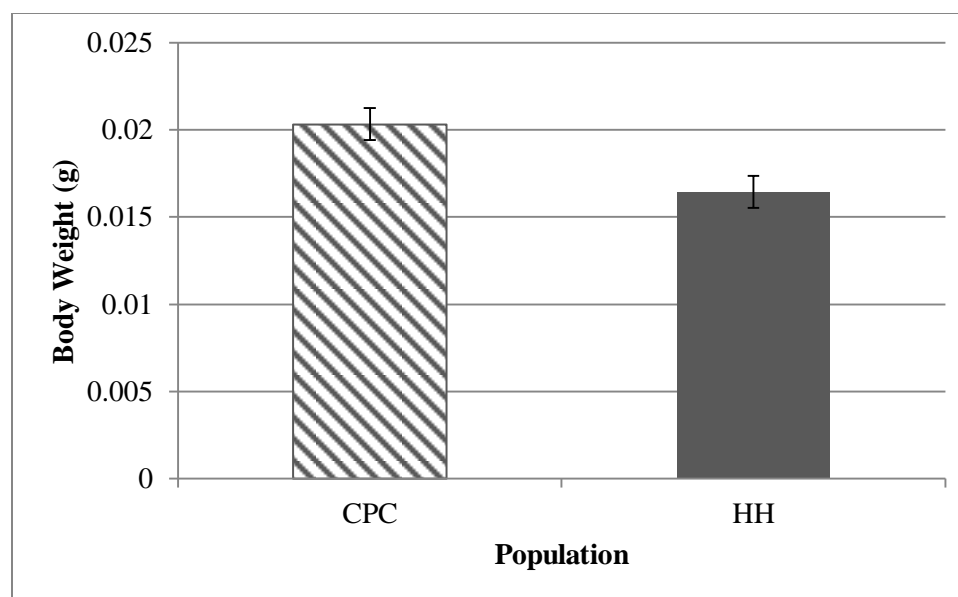


Figure 15. Body weight adjusted for a common shell weight for Carrying Place Cove (CPC) and Haycock Harbor (HH) *Littorina obtusata* used in the field growth experiment.

C. Water Temperature

a. Materials and Methods

HOBO Temp data loggers were placed in open containers with holes and were secured to bricks. One was put out at each site and covered with algae during the June collections. They were retrieved in July. Temperature readings were taken hourly for a total of 30 days. This corresponded to 55 high tides that were observed at both sites. To analyze the data, the three temperature readings closest to the time of the high tide were averaged and used as a single data point for the water temperature at that high tide.

T-tests were performed with an alpha value of 0.05 in Excel to test if the water temperature was significantly different between the two coves. Because of increased fluctuation of water temperature in certain portions, t-tests of three

approximately equal subsections of the temperature data were generated, to test if the significance held throughout.

b. Results

Water temperature at both coves increased slightly, about 2°C, over the course of the month (Figure 16). Temperatures at both coves followed a similar pattern of increasing, decreasing, and then increasing again (Figure 16). The most variation in water temperature was at the beginning of the data collection (Figure 16).

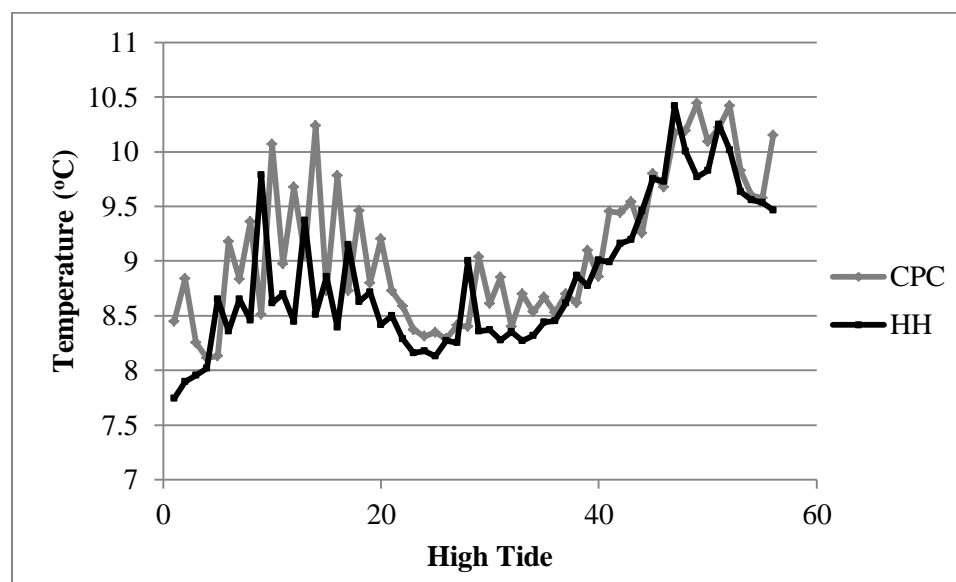


Figure 16. Average water temperature at high tide between 10 June and 10 July, 2013 at Carrying Place Cove and Haycock Harbor in Lubec, ME.

Examining the total range of water temperatures, the average water temperature at Carrying Place Cove was significantly higher than the temperature at Haycock Harbor ($p < 0.001$ $df = 54$). Splitting the data up, Carrying Place cove was significantly warmer in the first section of tides 2-19 ($p < 0.001$, $df = 17$),

during tides 20-38 ($p < 0.001$, $df = 18$), as well as during the last section of tides 39-56 ($p = 0.002$, $df = 17$).

CHAPTER 3. LABORATORY CRITICAL SIZE OF VULNERABILITY EXPERIMENTS

Prior to the laboratory experiments, *Littorina obtusata* and *Carcinus maenas* were collected from Carrying Place Cove and Haycock Harbor on 10-12 June, 2013 and on 9-10 July, 2013 during the morning and evening low tides. Until arrival back in Northampton, Massachusetts, *L. obtusata* and *C. maenas* were kept in labeled plastic containers, keeping individuals from different sites separate. These organisms were then used in the following experiments.

A. Foraging Experiments: critical size of vulnerability of *Littorina obtusata* to *Carcinus maenas* predation

a. Materials and Methods

Upon return to the laboratory, carapace width, right claw height, depth and length, as well as the left claw height of all of the right handed male *Carcinus maenas* from both sites were measured using digital calipers to (± 0.01 mm).

Feeding trials were conducted at Smith College over two-week time spans, from 17 – 27 June, and again from 15 – 25 July. These trials were designed to determine the critical size of vulnerability of *Littorina obtusata* and to compare the size scaling relationship between *C. maenas* and *L. obtusata* at different sites and time points. *C. maenas* were fed *L. obtusata* from their home site at two time points to test if the relative advantage that one organism has over the other differs over narrow spatial and temporal scales. Moreover, *C. maenas* were fed *L.*

obtusata from the other site to investigate if the outcome of the scaling relationship depends on a nuanced predator-prey interaction that would not otherwise be noticed.

Male *C. maenas* with a carapace width size range of 20.25 to 54.19 mm in June and 26.66 – 62.90 mm in July were used. The *L. obtusata* shell length ranges were 2.66 – 13.48 mm in June and 4.00 – 14.03 mm in July. In June, one fully regenerated left-handed *C. maenas* from each site was included. *C. maenas* were labeled individually and assigned to one of the four treatment combinations so that each treatment combination had a similar size range of *C. maenas*. Referring to Smith's (2004) study, based on *C. maenas* carapace width, three *L. obtusata* individuals within a 2-3 mm range in shell length were picked. *L. obtusata*'s shell length, as well as the lip thickness, were measured using digital calipers. *L. obtusata* shell lengths were approximately evenly spaced across the size 2-3 mm range. Each *C. maenas* was placed in an 800 ml translucent container with measurements of 9 cm in height and 11 cm in diameter that contained Crystal Sea™ brand artificial sea water with salinity between 32 and 35 ppt, aerated by an air-stone. The containers with *C. maenas* were put in an incubator set to 12°C with 15 hours of light and 9 hours of darkness to simulate summertime conditions at the collection site. In order to standardize *C. maenas*' hunger levels prior to the first feeding trial, the *C. maenas* were not fed for 24 hours. Three *L. obtusata* individuals were then put into each container and the container containing all four organisms was then returned to the incubator. After 24 hours,

the *L. obtusata* individuals were removed from the containers and were scored. Each *L. obtusata* specimen was classified as one of the following: crushed, chipped-dead, chipped-alive, probed, or okay. A fate of “crushed” indicated *C. maenas* crushed the *L. obtusata* shell and consumed the entirety of the *L. obtusata* soft body. A fate of “chipped-dead” indicated *C. maenas* chipped the *L. obtusata* shell without destroying it, and consumed the soft tissue. Similarly, a fate of “chipped-alive” indicated *C. maenas* chipped the shell without consuming or killing the organism. If the *L. obtusata* organism was “probed,” the soft body was removed from an intact shell. Finally, if the *L. obtusata* specimen was scored as “okay,” it was found with no signs of damage. The sizes for the next round of feeding were based on the previous trial’s results. If a *C. maenas* individual had crushed all of the *L. obtusata* individuals offered, the size range was increased, and if the *C. maenas* individual did not harm the *L. obtusata*, the size range was decreased. As in Smith’s (2004) study, a critical *L. obtusata* shell size was calculated by averaging the length of the largest *L. obtusata* the *C. maenas* individual successfully crushed and the length of the next larger *L. obtusata* the *C. maenas* was offered, but was chipped and unable to crush. In attempts to reduce the effects of *C. maenas* not eating because they were full, there was a 24 hour period between each feeding trial, when a new batch of *L. obtusata* within the adjusted size range was offered. If a *C. maenas* molted during the feeding trials, it was removed from the experiment. Once a difference of approximately 0.50 mm between the largest crushed *L. obtusata* and the smallest chipped *L. obtusata* was

recorded, an accurate critical size could be determined, and the *C. maenas* specimen was removed from all subsequent feeding trials. In total, there were five feeding trials in June and five feeding trials in July.

Carapace width and claw height were regressed to determine if they scaled similarly. Since they were similar, carapace width was chosen as the predator body size measurement (Appendix A, Figure 31). The \log_{10} [carapace width] was plotted against the \log_{10} [shell length] to generate the logarithmic translation of the scaling relationship.

b. Results

In June, the slopes of the scaling best fit lines including \pm one standard error for Carrying Place Cove and Haycock Harbor *Carcinus maenas* eating Haycock Harbor *Littorina obtusata*, as well as Carrying Place Cove *C. maenas* eating Carrying Place Cove *L. obtusata*, were less than the isometric scaling coefficient of 1.0. Haycock Harbor *C. maenas* eating Carrying Place Cove *L. obtusata* did not experience a significant advantage or disadvantage, as the slope \pm one standard error encompassed the isometric scaling coefficient 1.0 (Table 5; Figure 17). The ANCOVA indicated that the critical size of vulnerability, adjusted for *C. maenas* carapace width, did not differ as a function of the *C. maenas*' or *L. obtusata*'s location or their interaction in June (Table 6).

In July, the scaling relationship for Carrying Place Cove *C. maenas* eating Haycock Harbor *L. obtusata* and Haycock Harbor *C. maenas* eating Carrying Place Cove *L. obtusata* stayed relatively similar. Both of the scaling relationships

for *C. maenas* eating *L. obtusata* from their respective site experienced an increase, however only the scaling coefficient \pm one standard error for Haycock Harbor *C. maenas* eating Haycock Harbor *L. obtusata* exceeded 1.0 (Table 7; Figure 18). The ANCOVA indicated that the critical size of vulnerability, adjusted for *C. maenas* carapace width, did not differ as a function of the *C. maenas*' or *L. obtusata*'s location source or their interaction in July (Table 8).

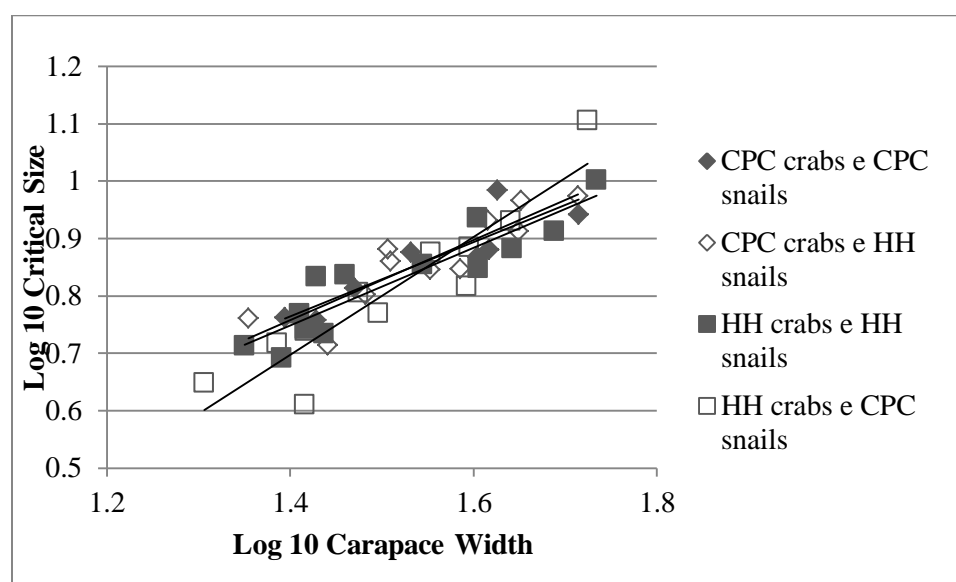


Figure 17. Size scaling of *Carcinus maenas* and *Littorina obtusata* in June for four treatments.

Table 5. June scaling coefficients \pm one standard error for *Carcinus maenas* and *Littorina obtusata*.

Slopes	-	+	Outcome
CPC e CPC	0.517548	0.779169	<i>L. obtusata</i>
CPC e HH	0.578676	0.812818	<i>L. obtusata</i>
HH e HH	0.583524	0.767526	<i>L. obtusata</i>
HH e CPC	0.882772	1.17054	equal

Table 6. Analysis of covariance for feeding trials in June for all four combinations.

Source	df	MS	F	P
Carapace Width	1	0.326596	149.7189	<.0001*
Crab Source	1	0.002242	1.028	0.317
Snail Source	1	0.000483	0.2215	0.6406
Crab Source * Snail Source	1	0.000368	0.1689	0.6834

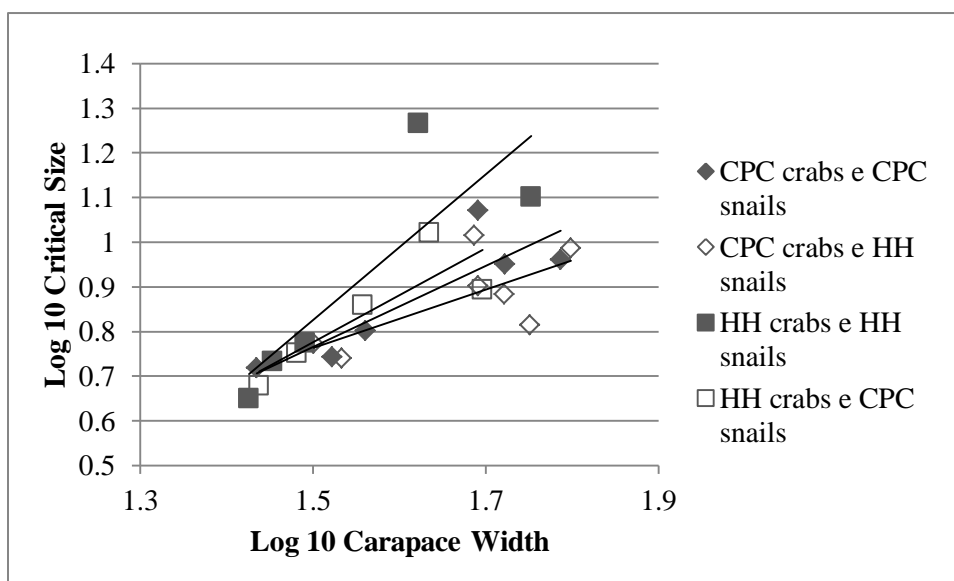


Figure 18. Size scaling of *Carcinus maenas* and *Littorina obtusata* in July for four treatments.

Table 7. July scaling coefficients \pm one standard error for *Carcinus maenas* and *Littorina obtusata*.

Slopes	-	+	Outcome
CPC e CPC	0.65058	1.16628494	Equal
CPC e HH	0.35760905	0.9570273	<i>L. obtusata</i>
HH e HH	1.02590888	2.23577056	<i>C. maenas</i>
HH e CPC	0.66167921	1.43096511	Equal

Table 8. Analysis of covariance for feeding trials in July for all four combinations.

Source	df	MS	F	P
Carapace Width	1	0.257252	46.3642	<.0001*
Crab Source	1	0.00259	0.4668	0.5037
Snail Source	1	0.010349	1.8651	0.1898
Crab Source * Snail Source	1	0.003521	0.6346	0.4366

B. Crushing Force: proxy for vulnerability

a. Materials and Methods

To determine site differences in the strength of *Littorina obtusata* shells, *L. obtusata* were crushed in an Instron machine as a proxy for *L. obtusata* vulnerability to predation (Trussel and Nicklin 2002). *L. obtusata* used in this experiment were collected in July and kept alive in tanks with *Ascophyllum* and chilled sea water. On 9 August, 2013 the *L. obtusata* were frozen for 15 minutes to kill them without disrupting the integrity of the shells. After the initial time in the freezer, the *L. obtusata* were kept on ice until they were tested on the Instron machine at Smith College. The Instron was set with a load cell rating of 500 N for a total load string minimum rating of 10 kN. One *L. obtusata* specimen at a time was placed aperture down onto the stationary, bottom compression platen, and the upper compression platen was lowered at a rate of 2 mm/min. When the *L. obtusata* shell cracked and failed, measured by a 40% change in force, the maximum load it experienced was recorded. This procedure was repeated for 25 individuals from each site, for a total of 50 times.

b. Results

There was an expected significant shell length effect: the longer the shell is, the more force it withstands ($p < 0.0001$). However, there was no difference in the force withstood by Carrying Place Cove and Haycock Harbor *L. obtusata* shells as measured by the Instron ($p = 0.8526$) (Figure 19).

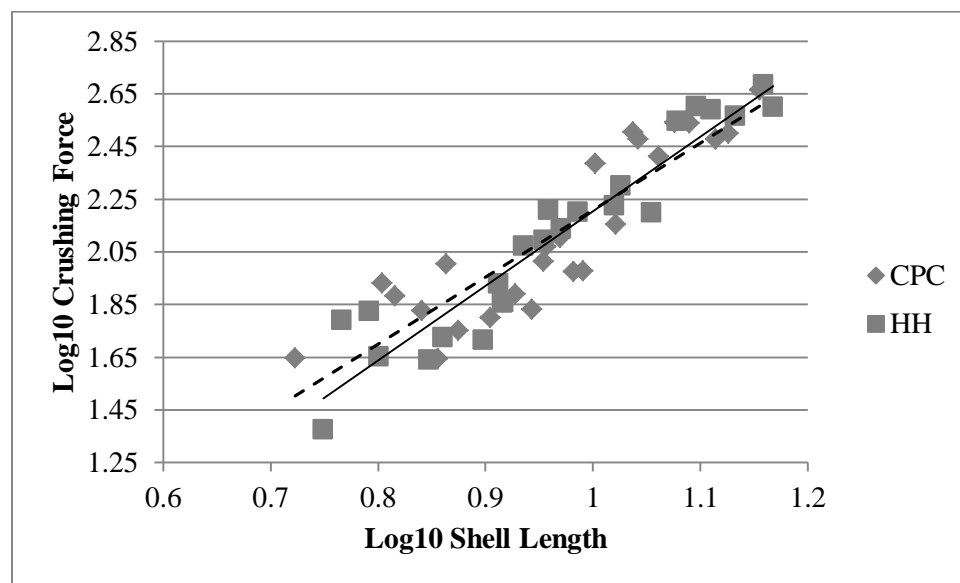


Figure 19. Crushing force needed for Carrying Place Cove (CPC) and Haycock Harbor (HH) *Littorina obtusata* shells to break plotted against shell length.

CHAPTER 4. MODELING

A. Lotka-Volterra Model: predator-prey population density behavior

a. Materials and Methods

To describe predator-prey behavior of *Carcinus maenas* and *Littorina obtusata*, a model with two nonlinear ordinary differential equations was constructed based on the Lotka-Volterra predator-prey model.

$$\text{(Equation 1a)} \quad \frac{ds}{dt} = a s \left(1 - \frac{s}{k}\right) - m_1 s c$$

$$\text{(Equation 1b)} \quad \frac{dc}{dt} = -b c + m_2 s c$$

Equation 1a, $\frac{ds}{dt}$, represents the growth function of *L. obtusata* population density. The first term, $a s \left(1 - \frac{s}{k}\right)$, is a logistic growth term, and the last term, $-m_1 s c$, models the detrimental effect of the predator-prey interaction. *L. obtusata* density is represented by s ; *C. maenas* density, by c . Equation 1b, $\frac{dc}{dt}$, represents the growth function of *C. maenas* population density in a predator-prey relationship. The first term in the *C. maenas* population equation, $-b c$, shows the density decrease of *C. maenas* when *L. obtusata* is not present. The second term, $m_2 s c$, shows the positive effect of the predator-prey interaction. (Again, *L. obtusata* density is represented by s ; *C. maenas* density, by c .)

The model includes five parameters. The parameters a and b relate to population growth (where a relates to *L. obtusata* growth, and b relates to *C.*

maenas growth). The parameter k is the carrying capacity of *L. obtusata*, and m_1 and m_2 both translate to how strong or weak the interaction term is.

With population density data that were collected in June and July of 2013, for each organism type in each site, in each case, there were two data points representing a population at $t = 0$ (June) and $t = 1$ (July). The data was scaled so that the *L. obtusata* population densities would be in snails/m² and the *C. maenas* population densities would be in units of crabs/minute. Using *Mathematica*, the least squares method for two-dimensional data was employed to find optimal parameter values to fit the model to the population data. With initial conditions dictated by the collected data, four population density vs. time curves were generated.

Parameter sensitivity analysis helps discern which parameters are crucial and which parameters are not. Parameter sensitivity was analyzed in *Mathematica* by looking at the differential for small t values, in turn assessing how the sum of the squares of the residuals (SQ) changes with respect to a change of a parameter. The smaller the differential is, the less effect that parameter has on the model. Equation 2 represents the sensitivity analysis for the case of parameter a , where LSQ stands for the least square function defined in the *Mathematica* code (Appendix B, Predator-Prey Model-Code).

$$\text{(Equation 2)} \quad \Delta SQ(a) = LSQ(a, b, k, m_1, m_2) - LSQ((a + t), b, k, m_1, m_2)$$

b. Results

Using the least squares method, values for the parameters a , b , m_1 , m_2 , and k were found for Carrying Place Cove in June and July, as well as for Haycock Harbor in June and July (Table 9).

Table 9. Parameter estimation using the least squares optimization for Carrying Place Cove and Haycock Harbor.

	a	b	m_1	m_2	k
Carrying Place Cove	11.2904	0.4471	0.0764	0.0144	88.3972
Haycock Harbor	7.6911	0.9280	0.0965	0.0503	123.4490

The parameters a , b , m_1 and m_2 had similarly large parameter sensitivities compared to k , which had the smallest influence in both Carrying Place Cove and Haycock Harbor equations (Table 10).

Table 10. Parameter sensitivity of parameters a , b , m_1 , m_2 , k using differentials and $t=0.000001$ for Carrying Place Cove and Haycock Harbor.

	a	b	m_1	m_2	k
Carrying Place Cove	-1.1243×10^{-5}	-4.2814×10^{-3}	-0.2564	-10.5657	-2.8276×10^{-7}
Haycock Harbor	-1.5575×10^{-4}	-1.5429×10^{-3}	-0.8235	-0.4297	-1.3108×10^{-8}

In the model for Carrying Place Cove, *Carcinus maenas* increased slightly in density and then leveled off to about 95 crabs/minute at time 4, corresponding to October (Figure 20). The *Littorina obtusata* population initially increased in the earlier portion of the summer and then stabilized at a lower density of 37 snails/m² (Figure 20).

The Haycock Harbor projection for *C. maenas* and *L. obtusata* both oscillate, tapering off to approximately 65 crabs/minute and 18 snails/m² respectively (Figure 21). In order to display the equilibrium behavior in the figure, the time span was increased unrealistically, since *C. maenas* and *L. obtusata* are spatially separated in the winter months, as previously mentioned.

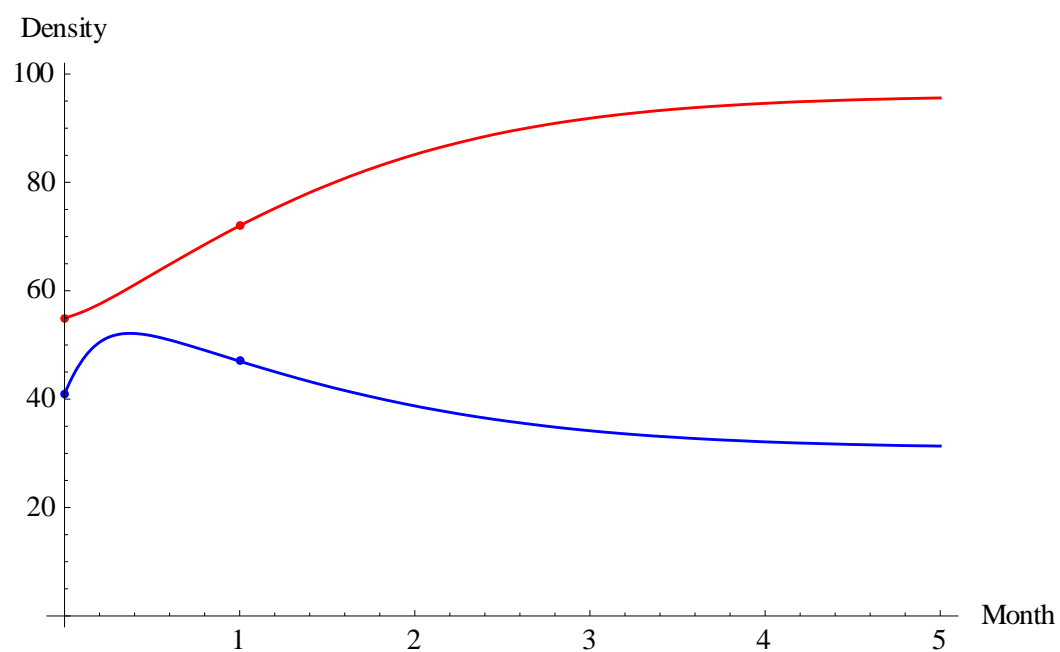


Figure 20. *Littorina obtusata* projected density over time for Carrying Place Cove shown in blue and *Carcinus maenas* density over time for Carrying Place Cove shown in red. Month 0 corresponds to June 2013; month 4 corresponds to October 2013. Months 0 and 1 were measured.

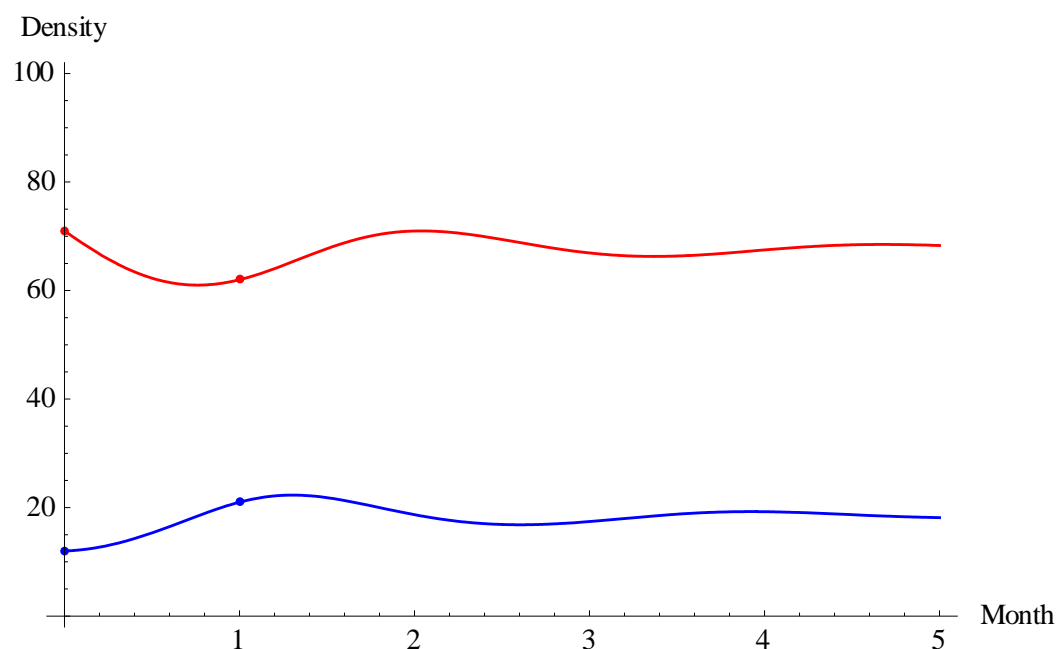


Figure 21. *Littorina obtusata* projected density over time for Haycock Harbor shown in blue, and *Carcinus maenas* density over time for Haycock Harbor shown in red. Month 0 corresponds to June 2013; month 10 corresponds to April 2014. Months 0 and 1 were measured.

B. Size Projections: predicted growth within size frequency distributions of *Littorina obtusata* populations

Only Carrying Place Cove data were used because a regression with a respectable R^2 value could not be produced with the Haycock Harbor data.

a. Materials and Methods

In attempt to tease out the effect of predation on different *Littorina obtusata* shell sizes, data based on individual shell growth from the field growth experiments were applied to size frequency distributions to obtain a predicted size frequency distribution. The prediction was then compared to the observed size frequency distribution for the corresponding month.

L. obtusata does not increase in shell length at the same rate throughout its lifetime. Smaller sized individuals grow at a relatively fast rate, in the middle size range, an inflection point is encountered, and above this size, *L. obtusata* individuals slow down linear growth and focus on increasing shell thickness (Nishida and Napompeth 1975). The upper size limit of *L. obtusata* in the Gulf of Maine and the Bay of Fundy is 15 mm (Kennedy 2009), and the associated inflection point is 7.5 mm. Based on this information, logistic growth of shell size was assumed, which implies relative growth rates $\frac{s'}{s}$ to be a linear function of s . The *L. obtusata* population size density projections created in this study assumed no outside factors affecting the population such as death by predation or other causes, and used equations in the form of $\frac{s'}{s} = a s + b$ on each. The variable s represents shell length, s' is the rate of change in shell length (growth), and a and b are constants that have a more tangible meaning in relation to each other. Information about shell size and growth can be extracted from such an equation, where $\frac{-b}{a}$ represents the maximum shell length and $\frac{-b}{2a}$ represents the size where the shell growth inflection point lies.

Projections of *L. obtusata* growth were obtained using measurements made during the *L. obtusata* field growth experiment. Bin size ranges were selected for approximately even distribution of the individuals. The average relative growth rate, $\left(\frac{SL_f - SL_i}{SL_i}\right)$, for *L. obtusata* in each bin was obtained by using calculations on the data completed prior to this analysis. SL_i stands for initial shell length and SL_f

stands for final shell length. Negative growth rates were discarded for this purpose, as they most likely were due to measurement inaccuracies, since negative growth is not viable for this species. A regression was performed on the growth rate against size categories in Excel to obtain a best fit line and an R^2 value.

The methods above were repeated with Carrying Place Cove data from 2010. The 2010 data were collected over three months, June, July, and August, and the relative growth rates were calculated based on the growth between June and August.

The logistic differential equations of shell growth generated were then applied, via a one-step Euler's method to the size frequency distributions of collected *L. obtusata* in June 2013 and 2010 to determine what the theoretical effect of shell growth on the population would be in July 2013 and 2010. Moreover, they were applied to the size frequency distributions of collected *L. obtusata* in July 2013 and 2010 to project backwards and predict what the size frequency distribution would have previously looked like in June 2013 and 2010. The equations were applied to only the July 2010 data to project forwards to predict what the August 2010 size frequency distribution would look like as well. As a measure of validity of the model, the same projections for the Carrying Place Cove 2013 size frequency distribution data with Carrying Place Cove equations were completed on Haycock Harbor 2013 size frequency distributions.

b. Results

The 2013 regression equation used in the projection model was $y = -0.0257x + 0.3554$ ($R^2=0.8254$), and the 2010 regression equation used in the projection model was $y = -0.0165x + 0.1848$ ($R^2=0.9204$). The maximum *Littorina obtusata* shell length at Carrying Place Cove, calculated with the 2010 and 2013 equations, produced maximum values of 11.2 mm and 13.3 mm respectively. This would correspond to inflection points at shell lengths of 5.6 mm and 6.7 mm. Although the largest *L. obtusata* individual found in any of the population surveys was 14.73 mm, larger than the calculated maximum, the estimation of the inflection point matched what was observed, as shifts in the frequencies around the 6 mm size bin were apparent from the size frequency distribution figures for Carrying Place Cove and Haycock Harbor.

Comparing the collected data in June to the projections of the June distribution from the July data over the whole range of *L. obtusata* shell lengths, the projections from both 2013 and 2010 models fit better for the larger shell lengths than for the smaller shell lengths. More individuals in the smaller ranges were predicted than observed. The 2013 and 2010 models fit similarly well, but the 2013 projections were closer to the collected values (Figure 22).

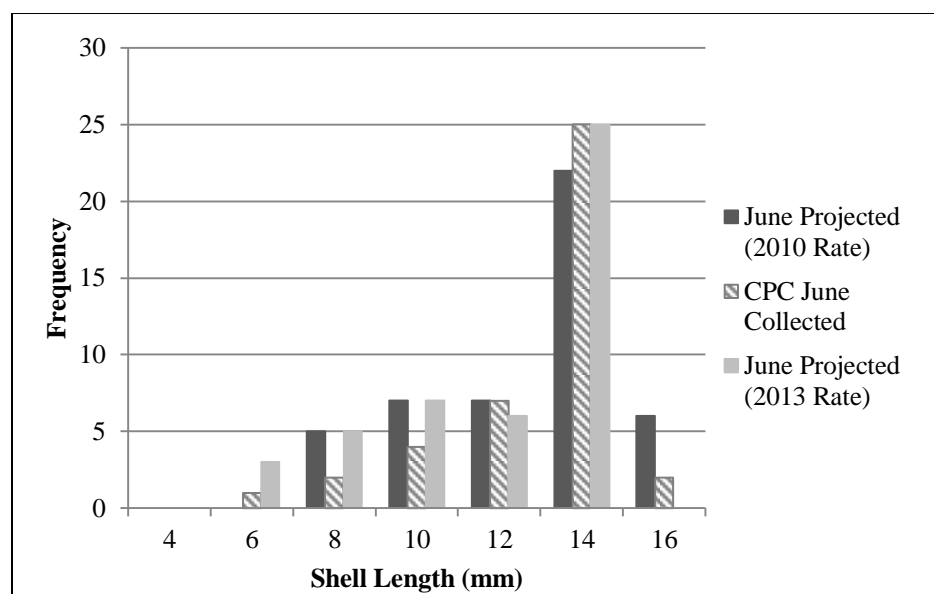


Figure 22. Comparison of *Littorina obtusata* frequencies from projections as well as actual June collected data at Carrying Place Cove in 2013.

Comparing the collected data in July to the projections of the July distribution from the June data over the whole range of *L. obtusata* shell lengths, the projections from both 2013 and 2010 models fit better for the larger shell lengths than for the smaller ones. Fewer individuals in the smaller ranges were predicted than observed. The projections using the 2010 model fit slightly better than the 2013 one, since the 2010 projections and the collected values are exactly the same for the 12 and 14 mm bins whereas the 2013 projections slightly differ from the collected values (Figure 23).

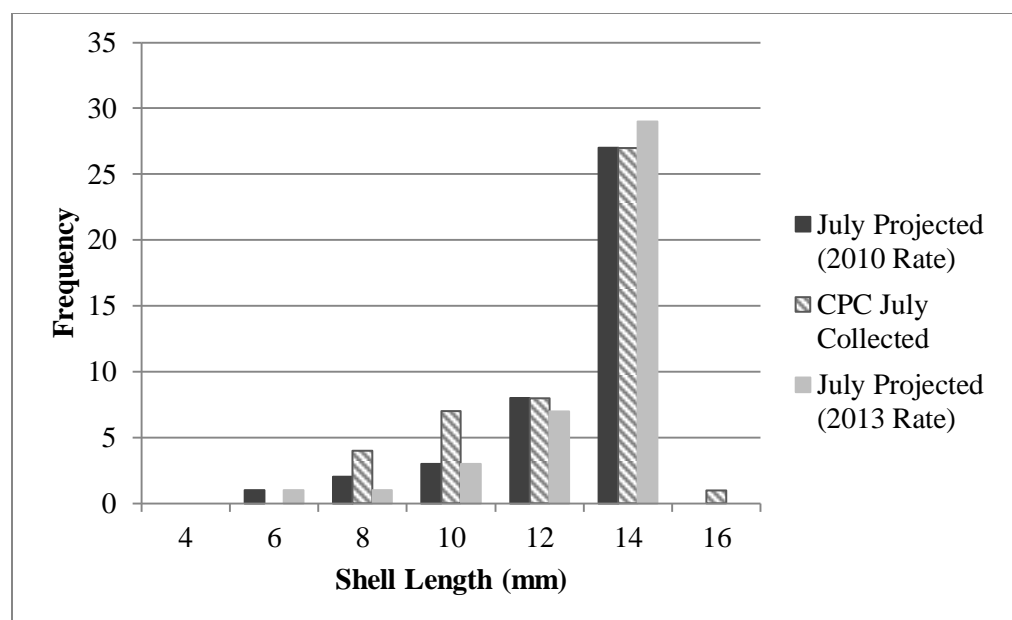


Figure 23. Comparison of *Littorina obtusata* frequencies from projections as well as actual July collected data at Carrying Place Cove in 2013.

Overall, for June, July and August 2010, the 2010 and 2013 projections did not match the collected size frequency distributions closely. There were discrepancies between observed and predicted values across the entire size range. The 2013 projections for the June 2010 data loosely fit the June 2010 collected data (Figure 24). The 2010 projections for the July 2010 data matched up to the July 2010 collected data fairly well (Figure 25). In August, it seems as if the projections are shifted over one bin size larger compared to the collected data (Figure 26).

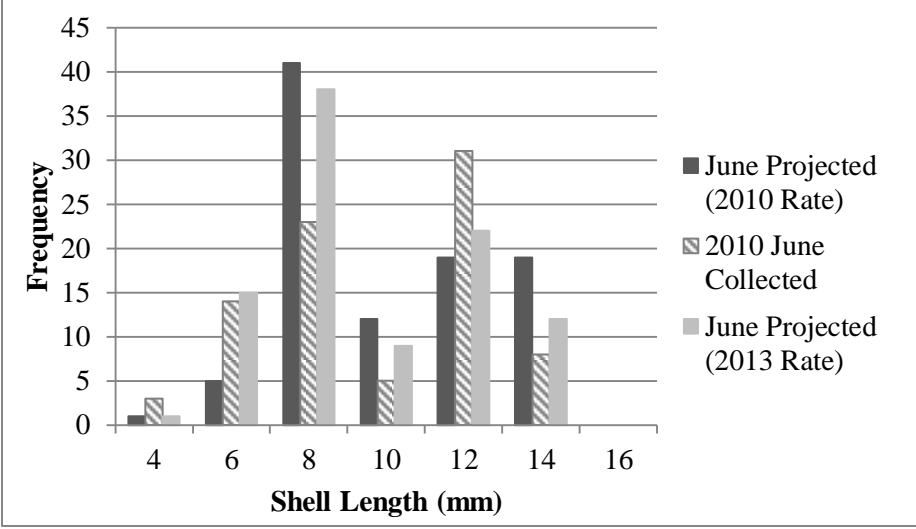


Figure 24. Comparison of *Littorina obtusata* frequencies from projections as well as actual June collected data at Carrying Place Cove in 2010.

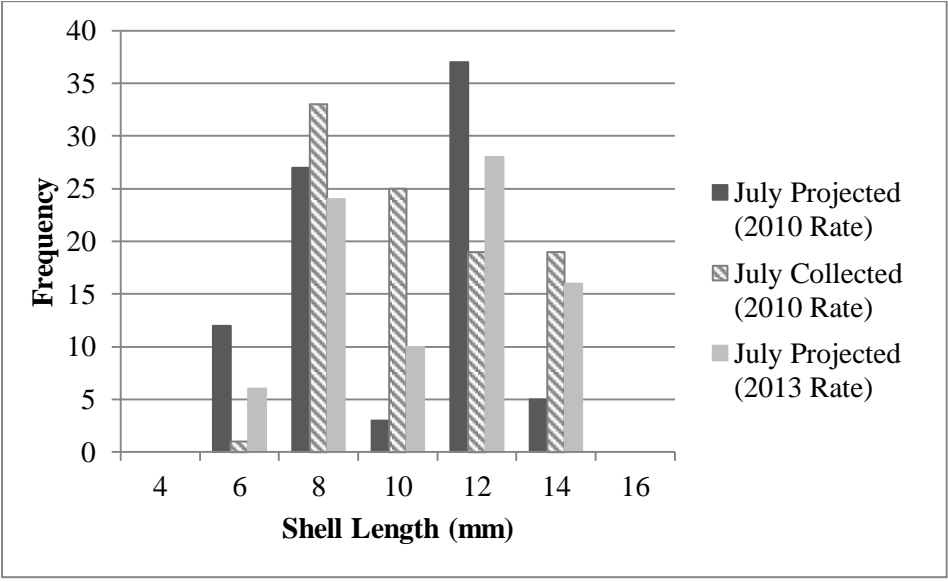


Figure 25. Comparison of *Littorina obtusata* frequencies from projections as well as actual July collected data at Carrying Place Cove in 2010.

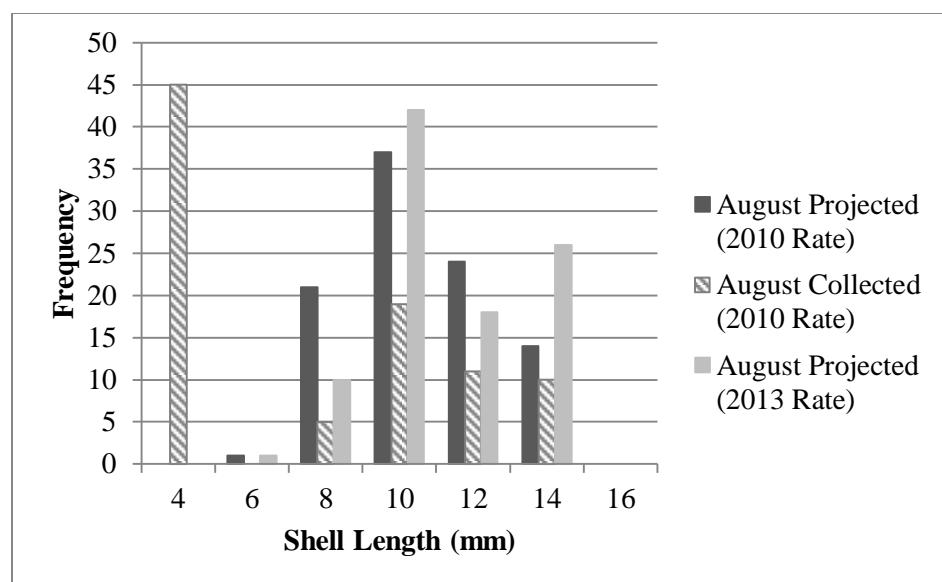


Figure 26. Comparison of *Littorina obtusata* frequencies from projections as well as actual August collected data at Carrying Place Cove in 2010.

For the June projections over the whole size range for Haycock Harbor using the Carrying Place Cove models compared to the June collected data, there were only large discrepancies in the lower size categories (Appendix A, Figure 32). The collected and the projected frequencies of *L. obtusata* in the 6 and 8 mm bins were very different, as the collected values were much greater than the projected values. The larger bins matched more closely. The 2010 projection was more accurate than the 2013 projection, as the frequencies were closer to the actual values. (Appendix A, Figure 32).

For the July projections over the whole size range for Haycock Harbor using the Carrying Place Cove models, the 2010 and the 2013 models only fit the collected data for the larger size categories (Appendix A, Figure 33). For the smaller bins, the projections vastly overestimated the actual July collected values.

C. *Littorina obtusata* Vulnerability to *Carcinus maenas* Predation:

population-level model

Critical size of vulnerability data for *Littorina obtusata* and size frequency distributions of both *Carcinus maenas* and *L. obtusata* were related to determine how vulnerable size classes of *L. obtusata* in the field were to *C. maenas* predation across narrow temporal and spatial scales. Both sites, Carrying Place Cove and Haycock Harbor, as well as both months, June and July, were examined, producing the following four conditions: Carrying Place Cove in June, Carrying Place Cove in July, Haycock Harbor in June, and Haycock Harbor in July.

a. Materials and Methods

To determine the portion of the *Littorina obtusata* population that was vulnerable to *Carcinus maenas* predation, the size scaling regressions from the critical size of vulnerability experiments were used (Table 11).

Table 11. Experimentally derived size scaling regression equations for *Carcinus maenas* and *Littorina obtusata* originating from the same site in June and July. The variable y represents \log_{10} [shell length] of *Littorina obtusata* and x represents \log_{10} [carapace width] of *Carcinus maenas*.

Treatment	Size Scaling Regression Equation
Carrying Place Cove, June	$y = 0.6484x - 0.1436$
Carrying Place Cove, July	$y = 0.9084x - 0.5965$
Haycock Harbor, June	$y = 0.6755x - 0.1970$
Haycock Harbor, July	$y = 1.6308x - 1.6206$

The absolute critical size of vulnerability for the *L. obtusata* population was calculated using these size scaling regression equations and the log-transformed

carapace width of the largest *C. maenas* individual found during the time searches. The portion of the *L. obtusata* population that was vulnerable was then determined by dividing the number of *L. obtusata* individuals found that were smaller than the critical size by the total number of individuals found at that site and time.

To relate frequency of *C. maenas* to *L. obtusata* and see differences in vulnerability within size categories, a vulnerability model was created in *Mathematica* (Appendix B, Vulnerability Model-Code). First, the measured populations of *C. maenas* and *L. obtusata* were sorted into size bins, giving the size frequency distributions. The *C. maenas* data was sorted based on carapace width, with bin intervals of 5 mm. The *L. obtusata* data were split up into bins based on shell length, each bin spanning 2 mm. The average carapace width and shell length were calculated for each bin. The $\log_{10}[\text{average}]$ for *C. maenas* was also determined because the aforementioned size scaling regressions generated from the feeding trials use logarithmic values of predator body size as inputs. The average *C. maenas* log-transformed carapace width for each bin was inserted into the size scaling regression to obtain the corresponding critical size of *L. obtusata* vulnerability. The critical size for each *C. maenas* bin was compared to the average *L. obtusata* shell length for each bin, creating a matrix of vulnerabilities. When given a choice, *C. maenas* eats prey in roughly the lower $\frac{1}{3}$ of the size range below the critical size to mitigate claw damage (Juanes 1992). Thus, *L. obtusata* falling within different portions of the critical size range face varying degrees of

predation. When determining vulnerability, if the average shell length was $\frac{1}{3}$ of the *C. maenas* critical size, the corresponding element of the matrix was allocated the value 1.0. Because preference would inherently be non-linear, if the *L. obtusata* shell length was between $\frac{1}{3}$ and $\frac{2}{3}$ of the critical size, a value of 0.5 was placed at that index of the vulnerability matrix. If the shell length was equal to or greater than $\frac{2}{3}$ of the critical size of vulnerability, the associated element of the matrix received a value of 0.25. Once this matrix was completed, individual *L. obtusata* vulnerabilities for each bin were calculated. Each element in the vulnerability matrix was multiplied by the corresponding frequency of *C. maenas* in that bin. These products were added up for each bin of *C. maenas* and the sum was divided by the frequency of *L. obtusata* in that particular bin, resulting in a relative vulnerability per *L. obtusata* individual. In terms of matrices and vectors, the calculated vulnerability for each size bin is as follows: $vulS = \frac{(V \cdot freqC)}{freqS}$, where *V* is the vulnerability matrix, *freqC* and *freqS* are the crab and snail frequencies, and the division is term by term.

When assessing the severity of vulnerability to predation, high vulnerability was defined as relative vulnerabilities per *L. obtusata* individual that were greater than 1.0. Moderate vulnerability was designated as relative vulnerabilities per *L. obtusata* individual that were less than 1.0 and greater than 0.0. If the vulnerability was 0.0, *L. obtusata* in that size category were larger than the critical size, thus obtaining a size refuge from *C. maenas*.

b. Results

The absolute critical size of vulnerability for each *Littorina obtusata* population increased at both sites between June and July, although there was a much greater difference between months at Haycock Harbor than at Carrying Place Cove (Table 12). This resulted in an increase in the portion of the population susceptible to predation over the short time span in question. Moreover, in both June and July, a greater portion of the Haycock Harbor *L. obtusata* population was vulnerable to predation than the Carrying Place Cove *L. obtusata* population (Table 12).

Table 12. Absolute critical size of vulnerability of *Littorina obtusata* to *Carcinus maenas* on a population level as well as the percent of the *Littorina obtusata* population that is vulnerable to predation.

	Critical Size (June)	Percent Vulnerable (June)	Critical Size (July)	Percent Vulnerable (July)
Carrying Place Cove	9.366 mm	15%	10.092 mm	26%
Haycock Harbor	8.203 mm	71%	17.304 mm	100%

As displayed by the vulnerability matrix for Carrying Place Cove in June, the three largest *L. obtusata* size classes, representing *L. obtusata* greater than 10 mm, were not vulnerable at all, consequently reaching a size refuge from *Carcinus maenas*. The smallest *L. obtusata* size class was the most vulnerable, as the average shell length was within all but the two smallest *C. maenas* categories' possible size range (Table 13; Figure 27 A).

Table 13. Matrix of vulnerability to *Carcinus maenas* for *Littorina obtusata* at Carrying Place Cove in June 2013.

	C_1	C_2	C_3	C_4	C_5	C_6	C_7	C_8	C_9	C_{10}
S_1	0	0	0.25	0.25	0.25	0.5	0.5	0.5	0.5	0.5
S_2	0	0	0	0	0	0.25	0.25	0.25	0.25	0.25
S_3	0	0	0	0	0	0	0	0	0	0.25
S_4	0	0	0	0	0	0	0	0	0	0
S_5	0	0	0	0	0	0	0	0	0	0
S_6	0	0	0	0	0	0	0	0	0	0

The relative vulnerability calculated for each *L. obtusata* size class, taking both predator and prey size frequency distributions into account, was lower for the larger *L. obtusata* size bins, mirroring the decrease in frequency by which that size *L. obtusata* was within the accessible size range of a particular *C. maenas* bin (Table 14; Figure 27 A).

Table 14. Relative vulnerabilities for individual size classes of *Littorina obtusata* at Carrying Place Cove in June 2013.

<i>L. obtusata</i> Size Range (mm)	Relative Vulnerability per <i>L. obtusata</i>
(4, 6]	10.75
(6,8]	1.875
(8,10]	0.125
(10, 12]	0
(12, 14]	0
(14, 16]	0

The *L. obtusata* at Carrying Place Cove in July were overall less vulnerable than the *L. obtusata* at Carrying Place Cove in June, as only four out of the ten *C. maenas* bins contained *C. maenas* that would theoretically be able to consume the *L. obtusata* present at that time and place (Table 15; Figure 27 B).

Table 15. Matrix of vulnerability to *Carcinus maenas* for *Littorina obtusata* at Carrying Place Cove in July 2013.

	C_1	C_2	C_3	C_4	C_5	C_6	C_7	C_8	C_9	C_{10}
S_1	0	0	0	0	0	0	0.25	0.25	0.25	0.25
S_2	0	0	0	0	0	0	0	0	0.25	0.25
S_3	0	0	0	0	0	0	0	0	0	0
S_4	0	0	0	0	0	0	0	0	0	0
S_5	0	0	0	0	0	0	0	0	0	0

The relative vulnerability, calculated for each *L. obtusata* size class at Carrying Place Cove in July, taking the size frequency distributions for both *C. maenas* and *L. obtusata* into account, followed a similar pattern, as one might expect, of the smallest *L. obtusata* being most vulnerable, and vulnerability decreasing with size (Table 16; Figure 27 B). The size refuge for Carrying Place Cove *L. obtusata* in July was achieved by the third size category, corresponding to *L. obtusata* greater than 10 mm.

Table 16. Relative vulnerabilities for individual size classes of *Littorina obtusata* at Carrying Place Cove in July 2013.

<i>L. obtusata</i> Size Range (mm)	Relative Vulnerability per <i>L. obtusata</i>
(6,8]	1.125
(8,10]	0.212
(10, 12]	0
(12, 14]	0
(14, 16]	0

Once again, at Haycock Harbor in June, the smaller *L. obtusata* were found to be more vulnerable than the larger ones, and invulnerability, due to size refuge, was observed for *L. obtusata* in the fourth size class or higher, translating to *L. obtusata* greater than 10 mm (Table 17; Figure 27 C). Every size category of *C.*

maenas found was theoretically able to consume individuals in the smallest *L. obtusata* category, which was unique to this site and time combination.

Table 17. Matrix of vulnerability to *Carcinus maenas* for *Littorina obtusata* at Haycock Harbor in June 2013.

	C_1	C_2	C_3	C_4	C_5	C_6
S_1	0.25	0.25	0.5	0	0.5	0.5
S_2	0	0	0.25	0	0.25	0.5
S_3	0	0	0	0	0	0.25
S_4	0	0	0	0	0	0
S_5	0	0	0	0	0	0
S_6	0	0	0	0	0	0

The relative vulnerability, calculated for each size class at Haycock Harbor in June when factoring in the size frequency distributions for both species of interest, exhibited the same pattern: the smaller the *L. obtusata* size class, the more vulnerable they were to predation by *C. maenas* (Table 18; Figure 27 C).

Table 18. Relative vulnerabilities for individual size classes of *Littorina obtusata* at Haycock Harbor in June 2013.

<i>L. obtusata</i> Size Range (mm)	Relative Vulnerability per <i>L. obtusata</i>
(2, 4]	7.5
(4,6]	0.286
(6,8]	0.036
(10, 12]	0
(12, 14]	0
(14, 16]	0

The Haycock Harbor size scaling regression equation increased considerably from June to July, which translated to all size classes of *L. obtusata* being vulnerable to *C. maenas* predation (Table 19; Figure 27 D). Although all *L.*

obtusata size bins were vulnerable, not all size bins of *C. maenas* contained individuals that were able to consume any of the *L. obtusata*.

Table 19. Matrix of vulnerability to *Carcinus maenas* for *Littorina obtusata* at Haycock Harbor in July 2013.

	C_1	C_2	C_3	C_4	C_5	C_6	C_7	C_8	C_9	C_{10}
S_1	0	0	0	0.25	0.25	0.5	0.5	0.5	1	1
S_2	0	0	0	0	0	0.25	0.25	0.5	0.5	0.5
S_3	0	0	0	0	0	0	0.25	0.25	0.5	0.5
S_4	0	0	0	0	0	0	0.25	0.25	0.5	0.5
S_5	0	0	0	0	0	0	0	0.25	0.25	0.25
S_6	0	0	0	0	0	0	0	0	0.25	0.25

The relative vulnerability calculated for each *L. obtusata* size class at Haycock Harbor in July was high for all size classes except for the largest and the one with the highest frequency (Table 20; Figure 27 D). The 8-10 mm bin was moderately vulnerable, due to the high frequency of *L. obtusata* in that category, and the 14-16 mm *L. obtusata* category was also moderately vulnerable because only the two largest *C. maenas* bins, each consisting of only one specimen, contained individuals that were theoretically capable of consuming them.

Table 20. Relative vulnerabilities for individual size classes of *Littorina obtusata* at Haycock Harbor in June 2013.

<i>L. obtusata</i> Size Range (mm)	Relative Vulnerability per <i>L. obtusata</i>
(4, 6]	11.75
(6,8]	6.5
(8,10]	0.85
(10, 12]	2.125
(12, 14]	1
(14, 16]	0.5

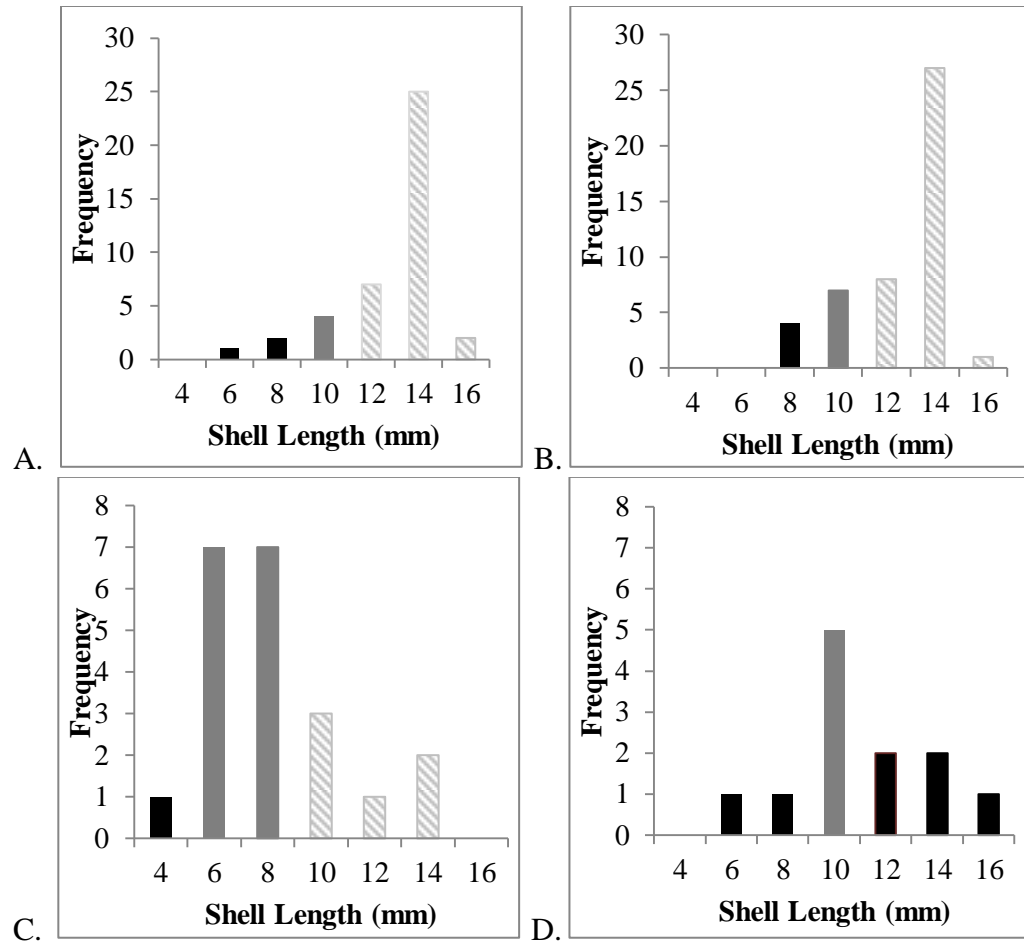


Figure 27 A-D. Size frequency distribution of *Littorina obtusata* indicating relative degrees of vulnerability (dark solid=most vulnerable, light solid=moderately vulnerable, hatched=invulnerable—size refuge) in June and July at Carrying Place Cove and Haycock Harbor. A) Carrying Place Cove, June. B) Carrying Place Cove, July. C) Haycock Harbor, June. D) Haycock Harbor, July.

CHAPTER 5. DISCUSSION

Differences in the size-scaling interactions of *Carcinus maenas* and *Littorina obtusata* were observed in the narrow temporal scale over which this study was conducted. Early in the season, in June, *C. maenas* is at a disadvantage, but then gains the upper hand in July. This temporal difference is most likely due to the differential growth strategies of the two combatants in the ‘arms race,’ as many individuals in the *C. maenas* populations at both sites molted within the time between experiments and consequently surpassing the linear *L. obtusata* growth. The growth strategies of the two combatants in the ‘arms race’ led to dynamic interactions within a short amount of time.

The predator-prey relationship varies over a narrow spatial scale as well. *L. obtusata* at Carrying Place Cove and at Haycock Harbor demonstrated different growth tactics, where Carrying Place Cove *L. obtusata* had thinner shells and larger body mass compared to *L. obtusata* at Haycock Harbor. This result, in conjunction with differences in size frequency distributions of both organisms, led to vulnerability predictions that varied over a narrow spatial scale.

Subtle differences between sites, such as *L. obtusata* shell thickness, shell shape and shell strength, as well as familiarity of the predator and prey may influence the outcome of the interaction. When *C. maenas* ate *L. obtusata* from the away site, it did not exhibit an increase in scaling factor benefiting *C. maenas*, but rather scaled similarly in June and July. When faced with prey from a foreign

site, the predator, *C. maenas*, reacted differently. This difference in handling could be due to subtleties of the *L. obtusata* shell properties, such as shape or thickness or exercised induced performance. *L. obtusata* at Carrying Place Cove grew more in shell length and height over the course of this study. *L. obtusata* at Haycock Harbor were thicker than their Carrying Place Cove counterparts, although the change in thickness was similar at both coves. Perhaps *C. maenas* originating from Carrying Place Cove are better suited to prey on *L. obtusata* with higher spired, and when faced with a thicker, lower spired individual, the *C. maenas* do not perform as well. Conversely, *C. maenas* from Haycock Harbor are used to, and thus may be better suited for thicker, lower spired *L. obtusata*, and when they attack a thinner shelled, higher spired *L. obtusata*, the *C. maenas* has an advantage because of exercise (Smith 2004).

Thinner shells, as well as higher spires are properties of snail shells that increase their vulnerability. Before the invasion of *C. maenas* to the East Coast of the United States, truly high spired and thin shell walled *L. obtusata* were often found along the coast. Now, *L. obtusata* with a high spire and a thin shell wall are rarely found. Since the invasion, the presence of the predator *C. maenas* has induced a phenotypically plastic response in *L. obtusata* to decrease vulnerability to predation (Trussell and Smith 2000). Seeley (1986) found experimentally that higher spired and thinner shell walled *L. obtusata* individuals were more vulnerable to predation than the lower spired, thicker shelled *L. obtusata*. A change in shell shape to reduce vulnerability to predation has also been observed

experimentally: when grown in a habitat with *C. maenas*, *L. obtusata* was shown to thicken its shell in response (Trussell and Smith 2000). Increasing shell thickness is not what *L. obtusata* ordinarily do if there were no heavy predation pressures present, because there are tradeoffs for doing so. Increasing shell thickness decreases its vulnerability to predators at the cost of slowing down body growth, which would keep the individual at a vulnerable size for a longer amount of time (Palmer 1981). This phenomenon was observed in the collected data; the thicker shelled *L. obtusata* at Haycock Harbor had smaller body masses, compared to the *L. obtusata* at Carrying Place Cove.

Temperature affected *L. obtusata* shell growth differently over a narrow spatial scale than what was previously found for growth over a large spatial scale. On a larger scale, comparing sites in Massachusetts and Maine, Trussell and Smith (2000) showed that the *L. obtusata* reared in warmer waters, Massachusetts, would be less vulnerable to *C. maenas* predation, because they possessed thicker shell walls than their counterparts in the colder water environment of Maine. This finding is opposite from what was found in this study, since the water temperature was significantly warmer at Carrying Place Cove, yet the *L. obtusata* were thinner than those at Haycock Harbor. Perhaps, since the difference in temperature on the narrow spatial scale of sites in Lubec, Maine, was small, the slight increase in temperature actually promoted the linear growth of *L. obtusata* and the laying down of calcium carbonate, whereas when the water temperatures were more different from each other, the *L. obtusata* had

an easier time laying down shell in the warmer waters. Another possible explanation would be that, within a limited range, water temperature is not an important causal factor in influencing shell growth, in comparison with other factors, such as the local history of predation pressure.

Crushing force, as measured by the Instron machine, may be good at indicating large differences between shell strength, but did not call attention to the nuanced differences in shell properties. Trussell and Nicklin (2002) showed that crushing force can be used as a proxy for gauging how much force a predator, like *C. maenas*, would need to crush the *L. obtusata* shell in order to gain access to the edible soft body. The forces needed to crush *L. obtusata* shells from both sites were not significantly different, indicating there should be no difference in *C. maenas* strength needed to crush the shells from Carrying Place Cove and Haycock Harbor. When taking the differences found between the shell weights and lip thicknesses from the field growth experiment into consideration, it became apparent that the crushing force may not be a fine enough simulation. As mentioned before, Carrying Place Cove *L. obtusata* had thinner shells, so the expected crushing force should be less than that for Haycock Harbor *L. obtusata*. The *L. obtusata* found at Carrying Place Cove also had higher spires than *L. obtusata* at Haycock Harbor, furthering the expectation that they would withstand less force than the *L. obtusata* from Haycock Harbor. Carrying Place Cove *L. obtusata*, compared to Haycock Harbor *L. obtusata* of a similar shell length, were found to be more vulnerable to *C. maenas* predation in the size-scaling

experiment. The Instron applied force on the shell in one direction, whereas in a real-life encounter between *C. maenas* and *L. obtusata*, the *C. maenas* would have to handle the *L. obtusata* shell, seeking to gain entry at the weakest point.

The size frequency distributions of *C. maenas* changed over the length of the study. In June, the size frequency distributions of *C. maenas* at both Carrying Place Cove and Haycock Harbor were skewed towards the smaller size categories, while in July the *C. maenas* size frequency distributions were skewed towards the larger size categories at both sites. This change in distribution is a good indication that many of the *C. maenas* individuals molted in the time in between data collection. This shift in size frequency distribution was also mirrored at Haycock Harbor for *L. obtusata*, although the sheer number of individuals at Haycock Harbor was lower than that at Carrying Place Cove, so the change in size frequency distribution of *L. obtusata* at Haycock Harbor could be attributed to an insufficiently large dataset. The bimodal population distribution of *L. obtusata* noted by Goodwin (1977) was not observed at either site in either month. Possibly, the frequencies of the *L. obtusata* were too low to observe such a feature.

For both species, their densities at both sites were similar in June and July, suggesting that there was no detectable new recruitment of either *C. maenas* or *L. obtusata*, and that similar populations were sampled. Based on the population densities, different density behaviors were predicted from the Lotka-Volterra based model. At Carrying Place Cove, the *C. maenas* population seems to exhibit

monotonic damping, and the *L. obtusata* population behavior is best described by damped oscillations. At Haycock Harbor, both species demonstrate damped oscillations that are offset from each other. These conclusions are rather tentative. Fitting a model to only two data points, which is what was collected, is quite arbitrary, as many trajectories can be fitted to two points. A larger data set, with collections over multiple years, would be necessary to gain reliable and useful information about the predator-prey population dynamics at Carrying Place Cove and Haycock Harbor.

The growth rates calculated for the size projection model were supported by the observed maximum shell sizes and inflection points because of the similarity to the known values. The largest *L. obtusata* specimen found was 14.73 mm, close to the upper size limit of 15 mm. The maximum calculated shell lengths were smaller than the observed or the actual upper size limit. However, when the data were separated into size bins, the calculated and observed inflection points and maximum sizes aligned fairly well. The minor inconsistencies between observed and calculated values could be due to the data used to calculate the growth rates, as well as to how the growth rates were calculated themselves. For instance, if more *L. obtusata* individuals over a wider size range were measured in the experiments or if, when calculating the growth rates, smaller bins were used, results similar to what was expected could have potentially been found.

The projection model was created in order to see if gaps or discrepancies in *L. obtusata* frequencies would become apparent when comparing projected values

with collected data. If predation of *L. obtusata* in the smaller size categories was important, lower frequencies in these size bins would have been expected and the model would have overshoot the true values. Because there would generally be a size refuge from *C. maenas* predation obtained by the larger *L. obtusata*, projections for the frequencies of the larger size categories were expected to be similar to the collected frequencies for that month.

The projections for June compared to the collected frequencies of *L. obtusata* in June showed that there was an unexpectedly low number of *L. obtusata* in the smaller size bins and a relatively good fit for the upper size bins, indicating the presence of an outside force acting on the smaller *L. obtusata* disproportionately, causing the smaller *L. obtusata* to appear at lower frequencies. Comparing the July data with the projected frequencies, more individuals in the smaller size range were collected than expected, which does not seem logical. Additionally, when comparing collected data to the projections for the other month based on these data, the projections looked more similar to the collected data from which they stemmed than to the collected data for the other month.

Because the frequencies of *L. obtusata* in the smaller bins are so low, collecting larger samples would have reduced the variability of the *L. obtusata* frequencies from month to month and produced more reliable projections. When comparing data, it is important to obtain enough data to ascertain that the variation is true variation and not just noise. Increased sample size, obtained by

sampling more quadrats and more transects, would be imperative to test the validity of the model.

Vulnerability on a population level, based on size frequency distributions of both *C. maenas* and *L. obtusata*, showed site differences as well as temporal differences. In general, the smaller *L. obtusata* size classes were more vulnerable to *C. maenas* predation, as their shell length was included in more *C. maenas* size ranges of consumable prey. In one case, however, Haycock Harbor *L. obtusata* in the (8, 10] bin were not as vulnerable as the rest of the *L. obtusata* found at that time and place because of the relatively high frequency of individuals in that size category compared to the other size categories for *L. obtusata*. In the vulnerability model, this factor reduced the probability of each individual in that size bin to be preyed upon by *C. maenas*.

Both sites, Carrying Place Cove and Haycock Harbor, displayed an increase in maximum critical size of vulnerability for the *L. obtusata* population from June to July. The difference in the critical size for the population between months was small at Carrying Place Cove compared to that at Haycock Harbor. The increase in critical size of vulnerability of the population, or in other words, the size at which *L. obtusata* gains a size refuge, could be due to the growth of *C. maenas*, as indicated in the size frequency distributions. A shift in *C. maenas* population towards larger sizes via discrete growth allows *C. maenas* to surpass the continuous linear growth of *L. obtusata*. Hence an increase in critical size of

vulnerability of the *L. obtusata* population calculated with the largest *C. maenas* individuals would be expected.

At Haycock Harbor there was a large vulnerability difference in the *L. obtusata* population between June and July. In June, there was a size refuge for the *L. obtusata*, but in July, all of the individuals found were theoretically vulnerable. This large increase in the vulnerability range is reflected in the great increase in the scaling coefficient at Haycock Harbor from June to July. Although logically it makes sense that there would be an increase in the scaling coefficient as well as in the vulnerability size range, such a large increase might also be due to poor data fitting, as many *C. maenas* individuals molted and had to be removed from the experiment, leading to a decrease in data points. The temporal variation in *L. obtusata* vulnerability on the population level at Haycock Harbor could also be due to low *L. obtusata* frequencies, compared to at Carrying Place Cove. Since there were overall much fewer individuals collected at Haycock Harbor than at Carrying Place Cove in June and July, a small difference in frequency could make a large impact on vulnerability calculations. More transects with more quadrats should be used in future work to collect *L. obtusata* size frequency distributions, so as to mitigate effects of a small dataset.

The model of vulnerability of the *L. obtusata* population generated results that contradicted results from the field growth experiment as well as the size-scaling experiment. The vulnerability model indicated that specimens from Haycock Harbor would be more vulnerable to *C. maenas* predation; however, the field

growth and the size-scaling experiments produced results suggesting that *L. obtusata* from Haycock Harbor would be less vulnerable than those from Carrying Place Cove, as they had lower spires and had thicker shell walls. The inconsistency between the vulnerability model and the previously mentioned experiments originates from the investigation of different parameters. The vulnerability model just takes *L. obtusata* shell length into account; whereas the size-scaling experiment indicated that fine differences in shell thickness and shape are important in the outcome of the predator-prey interaction. The size-scaling relationship of *C. maenas* and *L. obtusata* from the same site influenced the vulnerability model, since the equations used were taken directly from that experiment. However, variation in handling and shape were not explicitly included in the vulnerability model. Shell properties, such as thickness and shell height, could be incorporated into the model to relate linear size with other parameters of the *L. obtusata* shell so as to get a more accurate idea of the vulnerability to *C. maenas* predation.

Size-scaling relationships between *C. maenas* and *L. obtusata* in July might not have been as accurate as in June, since many *C. maenas* individuals molted during the experiment and were excluded from further feeding trials. This led to a smaller number of individual data points and weaker R^2 values in July than in June.

The incorporation of the vulnerability model into the projection model for *L. obtusata* populations would be a logical next step. The vulnerabilities produced

for each *L. obtusata* bin would be used to simulate predation in the projection model from month to month. Frequencies of *L. obtusata* in each size category would have an associated relative vulnerability which would be converted into a number between 0 and 1, where the most vulnerable size classes would have a lower number, indicating a smaller percent of the group continuing on to the next time point. Based on this vulnerability number, random individuals from each bin would be removed from the size frequency distribution data, simulating casualties due to predation. The projections would then be executed as before, but with fewer individuals in the population.

This investigation has shown that there was a subtle relationship between *C. maenas* and *L. obtusata*, as slight differences in shape were important in determining whether a combatant would gain a disproportionate advantage over the other or not. Do the *C. maenas* know the difference between a thin and a thick shell walled *L. obtusata*? Would there be a preference of one over the other? A choice experiment could be conducted, where *L. obtusata* individuals from both sites would be offered to *C. maenas* simultaneously to see if *L. obtusata* from one site would get eaten more than those from the other site.

The changes over time in the size-scaling interactions between *C. maenas* and *L. obtusata* could be attributed to the growth strategies of each organism. A shift in this interaction was observed over the span of one month, but would this be the case after two months or even after the summer? Repeating the size-scaling experiments over the warmer months that *C. maenas* and *L. obtusata* share the

rocky intertidal would allow for the monitoring of the size-scaling interactions over a longer period of time, still on a relatively narrow time scale.

As the mobility of people on the planet has increased, so has the frequency by which organisms are moved quickly and over long distances. Hence, introduced and invasive species are important to study in order to acquire knowledge about how to handle imminent invasions. *C. maenas* is a global invader and information about their invasion process and the predator-prey dynamics that ensue is vital in producing invasion management plans. The patchy population densities of *C. maenas* in northern Maine are similar to the patchy population densities indicative of invasion fronts, and thus, the models created based off of data collected in northern Maine can be used as a proxy. A possibility for future research directions would be to apply the models created in this study to other *C. maenas* invasion sites around the world. The relationship between *C. maenas* and a native prey, such as *L. obtusata*, could also be investigated at varying stages of invasion and establishment and compared, using the models for vulnerability and population projections detailed in this study.

APPENDIX A

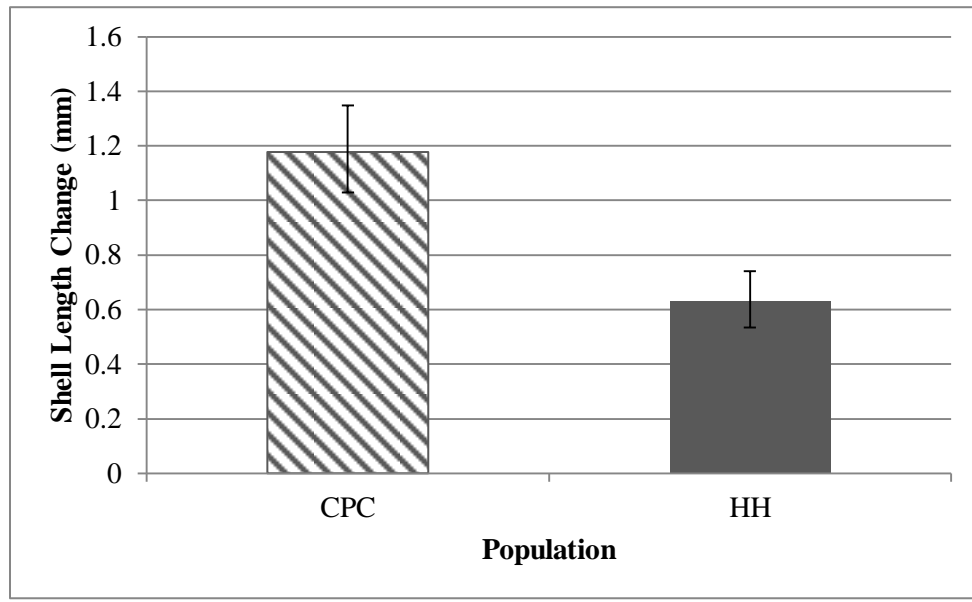


Figure 28. Change in shell length adjusted for a common initial shell length for Carrying Place Cove (CPC) and Haycock Harbor (HH) *Littorina obtusata* used in the field growth experiment.

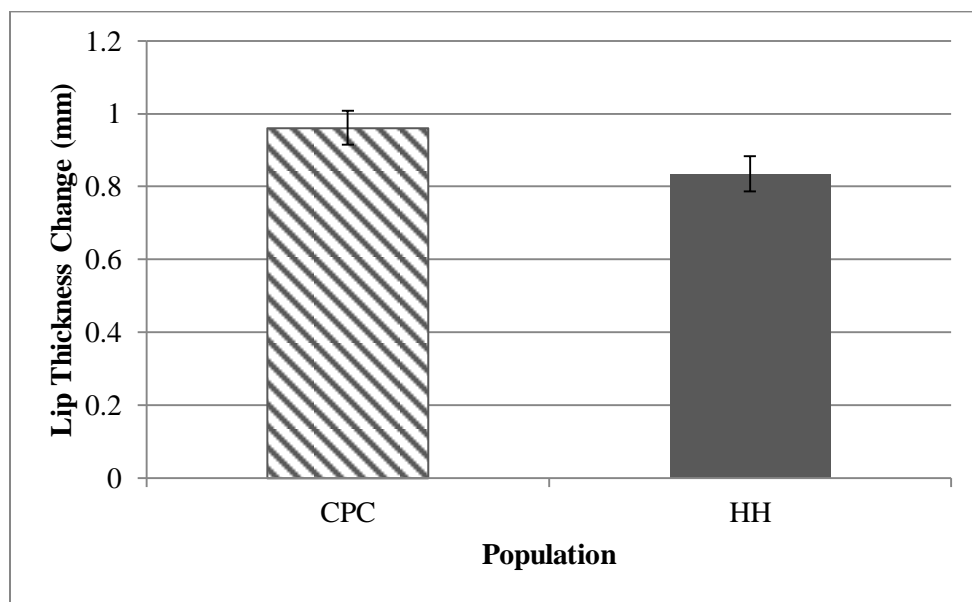


Figure 29. Change in lip thickness adjusted for a common initial shell length for Carrying Place Cove (CPC) and Haycock Harbor (HH) *Littorina obtusata* used in the field growth experiment.

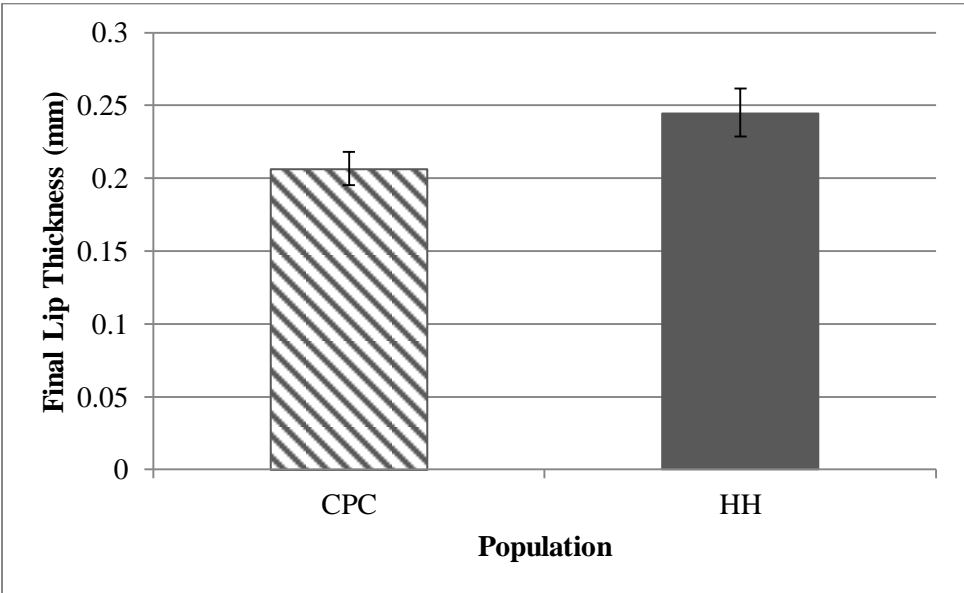


Figure 30. Final lip thickness adjusted for a common initial lip thickness for Carrying Place Cove (CPC) and Haycock Harbor (HH) *Littorina obtusata* used in the field growth experiment.

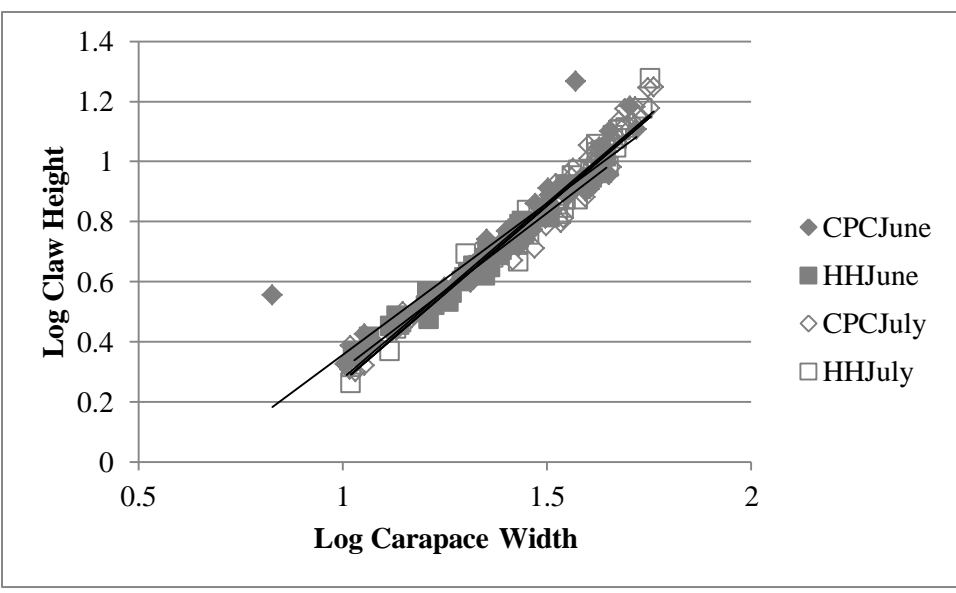


Figure 31. Scaling of *Carcinus maenas* carapace width and claw height for Carrying Place and Haycock Harbor in June and July.

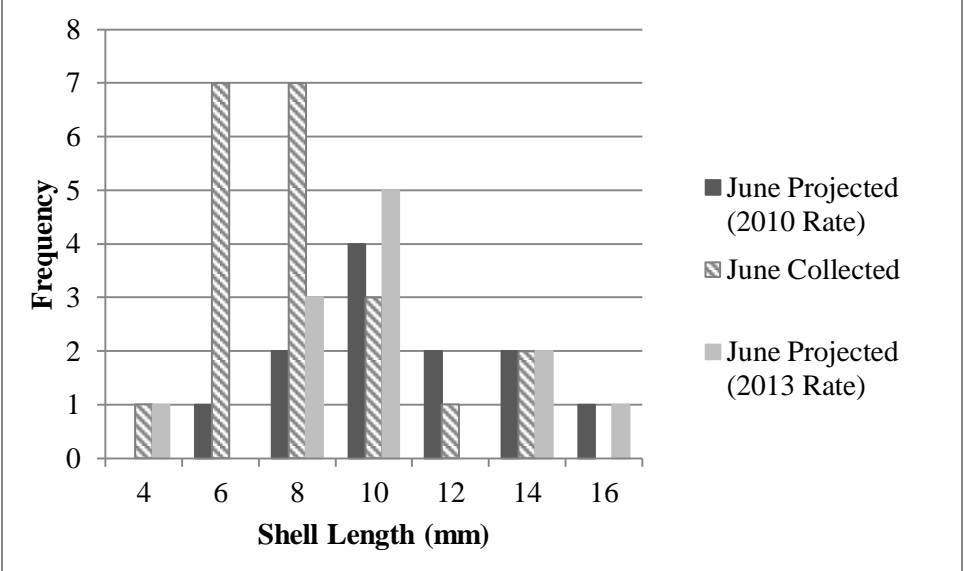


Figure 32. Comparison of *Littorina obtusata* frequencies from projections calculated based off of Carrying Place Cove growth rates as well as actual June collected data at Haycock Harbor in 2013.

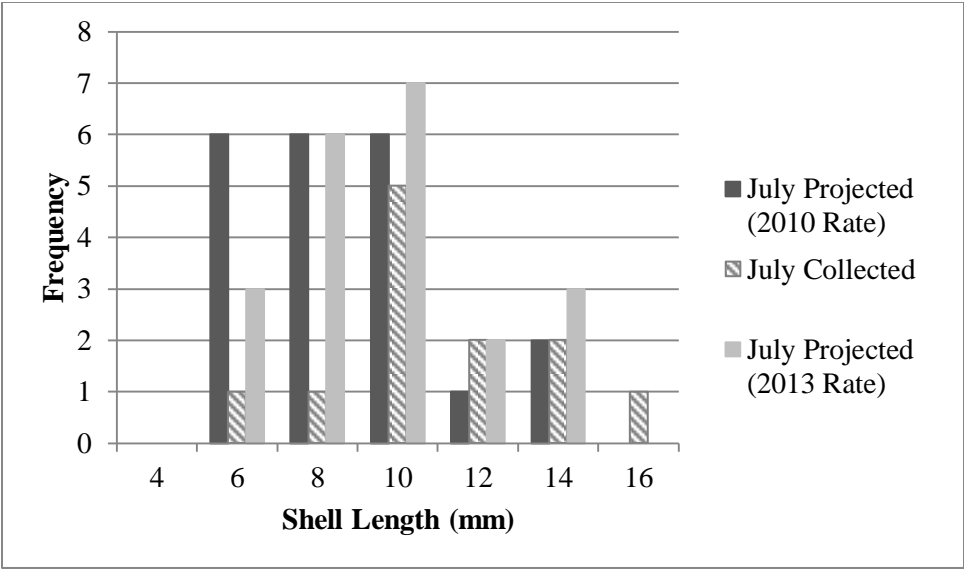


Figure 33. Comparison of *Littorina obtusata* frequencies from projections calculated based off of Carrying Place Cove growth rates as well as actual July collected data at Haycock Harbor in 2013.

APPENDIX B

PREDATOR-PREY MODEL-CODE:

Functions for *Littorina obtusata* (f) and *Carcinus maenas* (g)

```
f[c_,s_]:=a s (1-s/k)-m1 s c
g[c_,s_]:=-b c + m2 s c
```

Densities of both species at month 0=June and month 1=July for both sites

```
month = {0,1};
cpccrab = {55,72};
cpcsnail= {41,47};
hhcrab = {71,62};
hhsnail = {12,21};
```

Fitting Parameters for Carrying Place Cove:

Least squares function

```
lsqe[a_?NumberQ,b_?NumberQ,L_?NumberQ,m1_?NumberQ,m2_?
NumberQ]:=Module[{xsol,x},f[c_,s_]:=a s (1-s/k)-m1 s
c;
g[c_,s_]:=-b c+m2 s c;
```

Differential equations

```
eqpp={{c'[t]==g[c[t],s[t]],s'[t]==f[c[t],s[t]],s[0]==4
1,c[0]==55}};
```

Numerical solutions

```
{csol[t_],ssol[t_]}={c[t],s[t]}/.NDSolve[eqpp,{c,s},
{t,0,2}][[1]];
```

Fitting the parameters

```
Apply[Plus,(cpcsnail-(ssol[month]))^2+(cpccrab-
(csol[month]))^2]]
bf=FindMinimum[{lsqe[a,b,k,m1,m2]},{a,0.5,5},{b,0.5,5}
,{L,40,100},{m1,0.1,5},{m2,0.1,5}]
```

Parameter values found above

```
a=11.290456626187494`;b=0.4470655972576434`;k=88.39717
608018306`;m1=0.07638237948942453`;m2=0.01444329704086
4422`;
```

Behavior

```

eqpp={{c'[t]==g[c[t],s[t]],s'[t]==f[c[t],s[t]],s[0]==4
1, c[0]==55}};
{csol[t_],ssol[t_]}={c[t],s[t]}/.NDSolve[eqpp,{c,s},{t
,0,10}][[1]];
total[t_]={csol[t],ssol[t]};

```

Fitting Parameters for Haycock Harbor:**Least squares function**

```

lsqe[a_?NumberQ,b_?NumberQ,L_?NumberQ,m1_?NumberQ,m2_?
NumberQ]:=Module[{xsol,x},f[c_,s_]:=a s (1-s/k)-m1 s
c;
  g[c_,s_]:=-b c+m2 s c;

```

Differential equations

```

eqpp={{c'[t]==g[c[t],s[t]],s'[t]==f[c[t],s[t]],s[0]==1
2,c[0]==71}};

```

Numerical solutions

```

{csol[t_],ssol[t_]}={c[t],s[t]}/.NDSolve[eqpp,{c,s},{t
,0,5}][[1]];

```

Fitting the parameters

```

Apply[Plus,(hhsnail-(ssol[month]))^2+(hhcrab-
(csol[month]))^2]]
bf=FindMinimum[{lsqe[a,b,k,m1,m2]},{a,0.5,5},{b,0.5,5}
,{L,40,100},{m1,0.1,5},{m2,0.1,5}]

```

Parameter values found above

```

a=7.691140818051368`;b=0.9279944267334722`;k=123.44902
61153031`;m1=0.09649222599934545`;m2=0.050279264914244
89`;
f[c_,s_]:=a s (1-s/k)-m1 s c;
g[c_,s_]:=-b c+m2 s c;

```

Behavior

```

eqpp={{c'[t]==g[c[t],s[t]],s'[t]==f[c[t],s[t]],s[0]==1
2,c[0]==71}};
{csol[t_],ssol[t_]}={c[t],s[t]}/.NDSolve[eqpp,{c,s},{t
,0,10}][[1]];
total[t_]={csol[t],ssol[t]};

```

Parameter Sensitivity for both Carrying Place Cove and Haycock Harbor:

Small change in parameter a :

$$\frac{(\text{lsqe}[a, b, k, m1, m2] - \text{lsqe}[(a+0.000001), b, k, m1, m2])}{0.000001}$$

Small change in parameter b :

$$\frac{(\text{lsqe}[a, b, k, m1, m2] - \text{lsqe}[a, (b+0.000001), k, m1, m2])}{0.000001}$$

Small change in parameter k :

$$\frac{(\text{lsqe}[a, b, k, m1, m2] - \text{lsqe}[a, b, (k+0.000001), m1, m2])}{0.000001}$$

Small change in parameter m_1 :

$$\frac{(\text{lsqe}[a, b, k, m1, m2] - \text{lsqe}[a, b, k, (m1+0.000001), m2])}{0.000001}$$

Small change in parameter m_2 :

$$\frac{(\text{lsqe}[a, b, k, m1, m2] - \text{lsqe}[a, b, k, m1, (m2+0.000001)])}{0.000001}$$

VULNERABILITY MODEL-CODE:

Importing crab and snail size frequency data from the quadrats and the time searches.

```

path = ToString[NotebookDirectory[]];
S6CPC = Import[path<>"cpc_lobtusata_june.xlsx"];
S6CPC = Flatten[ S6CPC];
path = ToString[NotebookDirectory[]];
C6CPC = Import[path<>"cpc_cmaenas_june.xlsx"];
C6CPC = Flatten[ C6CPC];
path = ToString[NotebookDirectory[]];
S6HH = Import[path<>"hh_lobtusata_june.xlsx"];
S6HH= Flatten[ S6HH];
path = ToString[NotebookDirectory[]];
C6HH = Import[path<>"hh_cmaenas_june.xlsx"];
C6HH= Flatten[ C6HH];
path = ToString[NotebookDirectory[]];
S7CPC = Import[path<>"cpc_lobtusata_july.xlsx"];
S7CPC = Flatten[ S7CPC];
path = ToString[NotebookDirectory[]];
C7CPC = Import[path<>"cpc_cmaenas_july.xlsx"];
C7CPC = Flatten[ C7CPC];
path = ToString[NotebookDirectory[]];
S7HH = Import[path<>"hh_lobtusata_july.xlsx"];
S7HH= Flatten[ S7HH];
path = ToString[NotebookDirectory[]];
C7HH = Import[path<>"hh_cmaenas_july.xlsx"];
C7HH= Flatten[ C7HH];

```

Sort the imported data from smallest to largest shell length or carapace width.

```

S6CPC=Sort[S6CPC];
C6CPC=Sort[C6CPC];
S6HH=Sort[S6HH];
C6HH=Sort[C6HH];
S7CPC=Sort[S7CPC];
C7CPC=Sort[C7CPC];
S7HH=Sort[S7HH];
C7HH=Sort[C7HH];
Length[S6CPC];
Length[C6CPC];
Length[S6HH];
Length[C6HH];
Length[S7CPC];
Length[C7CPC];
Length[S7HH];

```

```
Length[C7HH];
```

Carrying Place Cove in June:

Sort the snail size frequency distribution data into size bins:

```
binlistS6CPC = BinLists[S6CPC, {Range[4,16,2]}]
```

Take the average shell length for each bin.

```
avgS6CPC=Map[Mean, binlistS6CPC];
```

Sort the crab size frequency distribution data into size bins.

Take the average carapace width for each bin.

Log-transform the averages.

```
binlistC6CPC = BinLists[C6CPC, {Range[5, 55, 5]}];
```

```
avgC6CPC = Map[Mean, binlistC6CPC];
```

```
logavgC6CPC = Log10[avgC6CPC];
```

Regression equation from size-scaling experiment for CPC crabs eating CPC snails in June.

```
CritSize6CPC[x_] := 0.6484*x - 0.1436
```

Generate critical sizes for each crab bin size. If there are no crabs in that bin, let that spot be 0.

```
critsize6CPC=Table[If[Length[binlistC6CPC[[k]]]==0,0,1  
0^(CritSize6CPC[logavgC6CPC][[k]]), {k,  
Length[binlistC6CPC]}];
```

Fill in a matrix of vulnerabilities. If the critical size is smaller than the snail shell length, then put a 0 (invulnerable). If the shell length falls in the smallest third of the critical size range, put a 1 (most vulnerable). If the shell length is in the middle third of the critical size range, put a 0.5 (medium vulnerability). If the shell length is in the largest third of the critical size range, put a 0.25 (least vulnerable).

```
CS6CPC=Table[Which[avgS6CPC[[k]]>critsize6CPC[[j]], 0,  
(2/3)*critsize6CPC[[j]]≤ avgS6CPC[[k]], 0.25,  
(1/3)*critsize6CPC[[j]]≤ avgS6CPC[[k]] && (2/3)*  
critsize6CPC[[j]]>avgS6CPC[[k]], 0.5, True, 1],  
{k,1,Length[avgS6CPC]}, {j,1,Length[critsize6CPC]}]
```

Calculate the frequency of each size bin for crabs and snails.

```
freqC6CPC1=Map[Length, binlistC6CPC][[1]];
freqC6CPC2=Map[Length, binlistC6CPC][[2]];
freqC6CPC3=Map[Length, binlistC6CPC][[3]];
freqC6CPC4=Map[Length, binlistC6CPC][[4]];
freqC6CPC5=Map[Length, binlistC6CPC][[5]];

```

```

freqC6CPC6=Map[Length, binlistC6CPC][[6]];
freqC6CPC7=Map[Length, binlistC6CPC][[7]];
freqC6CPC8=Map[Length, binlistC6CPC][[8]];
freqC6CPC9=Map[Length, binlistC6CPC][[9]];
freqC6CPC10=Map[Length, binlistC6CPC][[10]];

```

```

freqS6CPC1=Map[Length, binlistS6CPC][[1]];
freqS6CPC2=Map[Length, binlistS6CPC][[2]];
freqS6CPC3=Map[Length, binlistS6CPC][[3]];
freqS6CPC4=Map[Length, binlistS6CPC][[4]];
freqS6CPC5=Map[Length, binlistS6CPC][[5]];
freqS6CPC6=Map[Length, binlistS6CPC][[6]];

```

Calculate relative vulnerabilities: multiply the number in the vulnerability matrix by the frequency of crabs in the associated column. Add all of the elements in the row for a particular snail bin size up, and divide by the snail frequency in the associated bin.

```

VulS6CPC1=(CS6CPC [[1,1]]*freqC6CPC1+CS6CPC
[[1,2]]*freqC6CPC2+CS6CPC [[1,3]]*freqC6CPC3+CS6CPC
[[1,4]]*freqC6CPC4+CS6CPC [[1,5]]*freqC6CPC5+CS6CPC
[[1,6]]*freqC6CPC6+CS6CPC [[1,7]]*freqC6CPC7+CS6CPC
[[1,8]]*freqC6CPC8+CS6CPC [[1,9]]*freqC6CPC9+CS6CPC
[[1,10]]*freqC6CPC10)/freqS6CPC1

```

```

VulS6CPC2=(CS6CPC [[2,1]]*freqC6CPC1+CS6CPC
[[2,2]]*freqC6CPC2+CS6CPC [[2,3]]*freqC6CPC3+CS6CPC
[[2,4]]*freqC6CPC4+CS6CPC [[2,5]]*freqC6CPC5+CS6CPC
[[2,6]]*freqC6CPC6+CS6CPC [[2,7]]*freqC6CPC7+CS6CPC
[[2,8]]*freqC6CPC8+CS6CPC [[2,9]]*freqC6CPC9+CS6CPC
[[2,10]]*freqC6CPC10)/freqS6CPC2

```

```

VulS6CPC3=(CS6CPC [[3,1]]*freqC6CPC1+CS6CPC
[[3,2]]*freqC6CPC2+CS6CPC [[3,3]]*freqC6CPC3+CS6CPC
[[3,4]]*freqC6CPC4+CS6CPC [[3,5]]*freqC6CPC5+CS6CPC
[[3,6]]*freqC6CPC6+CS6CPC [[3,7]]*freqC6CPC7+CS6CPC
[[3,8]]*freqC6CPC8+CS6CPC [[3,9]]*freqC6CPC9+CS6CPC
[[3,10]]*freqC6CPC10)/freqS6CPC3

```

```

VulS6CPC4=(CS6CPC [[4,1]]*freqC6CPC1+CS6CPC
[[4,2]]*freqC6CPC2+CS6CPC [[4,3]]*freqC6CPC3+CS6CPC
[[4,4]]*freqC6CPC4+CS6CPC [[4,5]]*freqC6CPC5+CS6CPC
[[4,6]]*freqC6CPC6+CS6CPC [[4,7]]*freqC6CPC7+CS6CPC
[[4,8]]*freqC6CPC8+CS6CPC [[4,9]]*freqC6CPC9+CS6CPC
[[4,10]]*freqC6CPC10)/freqS6CPC4

```

```

VulS6CPC5=(CS6CPC [[5,1]]*freqC6CPC1+CS6CPC
[[5,2]]*freqC6CPC2+CS6CPC [[5,3]]*freqC6CPC3+CS6CPC
[[5,4]]*freqC6CPC4+CS6CPC [[5,5]]*freqC6CPC5+CS6CPC

```

```

[[5,6]]*freqC6CPC6+CS6CPC [[5,7]]*freqC6CPC7+CS6CPC
[[5,8]]*freqC6CPC8+CS6CPC [[5,9]]*freqC6CPC9+CS6CPC
[[5,10]]*freqC6CPC10)/freqS6CPC5
Vuls6CPC6=(CS6CPC [[6,1]]*freqC6CPC1+CS6CPC
[[6,2]]*freqC6CPC2+CS6CPC [[6,3]]*freqC6CPC3+CS6CPC
[[6,4]]*freqC6CPC4+CS6CPC [[6,5]]*freqC6CPC5+CS6CPC
[[6,6]]*freqC6CPC6+CS6CPC [[6,7]]*freqC6CPC7+CS6CPC
[[6,8]]*freqC6CPC8+CS6CPC [[6,9]]*freqC6CPC9+CS6CPC
[[6,10]]*freqC6CPC10)/freqS6CPC6

```

This code was repeated for Carrying Place Cove in July, Haycock Harbor in June, and Haycock Harbor in July. The following regression equations were used for each of the three other cases.

Carrying Place Cove crabs eating Carrying Place Cove snails in July:

CritSize7CPC[x_] := 0.9084*x - 0.5965

Haycock Harbor crabs eating Haycock Harbor snails in June:

CritSize6HH[x_] := 0.6755*x - 0.197

Haycock Harbor crabs eating Haycock Harbor snails in June:

CritSize7HH[x_] := 1.6308*x - 1.6206

WORKS CITED

- Ahyong, S. T. 2005. Range extension of two invasive crab species in eastern Australia: *Carcinus maenas* (Linnaeus) and *Pyromaia tuberculata* (Lockington). *Marine pollution bulletin*:460.
- Carlton, J. T., and A. N. Cohen. 2003. Episodic global dispersal in shallow water marine organisms: the case history of the European shore crabs *Carcinus maenas* and *C. aestuarii*. *Journal of Biogeography* 30:1809-1820.
- Carson, R., and S. Hubbell. 1998. *The edge of the sea / Rachel Carson; with illustrations by Bob Hines and a new introduction by Sue Hubbell*. Boston, Mass.: Houghton Mifflin Co., 1998; 1st Mariner Books ed.
- Cohen, A. N., J. T. Carlton, and M. C. Fountain. 1995. Introduction, dispersal and potential impacts of the green crab *Carcinus maenas* in San Francisco Bay, California. *Marine Biology*:225.
- Compton, T. J., J. R. Leathwick, and G. J. Inglis. 2010. Thermogeography predicts the potential global range of the invasive European green crab (*Carcinus maenas*). *Diversity & Distributions* 16:243-255.
- Davis, M. A. 2009. *Invasion biology [electronic resource] / Mark A. Davis*. Oxford; New York: Oxford University Press, 2009.
- Dow, R. L., and D. E. Wallace. 1952. Observations on green crabs (*C. maenas*) in Maine. Fisheries Circular No. 8, Bulletin of the Department of Sea and Shore Fisheries, Augusta, Maine USA.
- Emerson, S.B., H.W. Greene, and E.L. Charnov. 1994. Allometric aspects of predator-prey interactions. *Complex Organismal Functions: Integration and Evolution in Vertebrates*. Wiley and Sons, New York. 123-139.
- Forsman, A. 1996. Body size and net energy gain in gape-limited predators: a model. *Journal of Herpetology*:307.
- Goodwin, B. J. 1978. The growth and breeding cycle of *Littorina Obtusata* (Gastropoda: Prosobranchiata) from Cardigan Bay. *Journal of Molluscan Studies* 44:231.
- Juanes, F. 1992. Why do decapod crustaceans prefer small-sized molluscan prey? *Marine Ecology Progress Series* 87:239-249.

- Kennedy, M. 2009. *Littorina obtusata* (Linnaeus, 1758). World Register of Marine Species.
<www.marinespecies.org/aphia.php?p=taxdetails&id=140263>
- Lippert, K. A., J. M. Gunn, and G. E. Morgan. 2007. Effects of colonizing predators on yellow perch (*Perca flavescens*) populations in lakes recovering from acidification and metal stress. *Canadian Journal of Fisheries & Aquatic Sciences* 64:1413-1428.
- MacArthur, R. H., and E. R. Pianka. 1966. On optimal use of a patchy environment. *The American Naturalist*:603.
- Nishida, T., and B. Napompeth. 2009. Effect of age-specific predation on age distribution and survival of the giant African snail, *Achatina fulica*. *Hawaiian Entomological Society*: 22:119-123.
- Paine, R. T. 1976. Size-limited predation: An observational and experimental approach with the *Mytilus-Pisaster* interaction. *Ecology* 57:858.
- Palmer, A. R. 1990. Predator size, prey size, and the scaling of vulnerability: hatchling gastropods vs. barnacles. *Ecology* :759.
- Palmer, A. R. 1981. Do carbonate skeletons limit the rate of body growth. *Nature* 292:150.
- Rangeley, R. W., and M. L. H. Thomas. 1987. Predatory behaviour of juvenile shore crab *Carcinus maenas* (L.). *Journal of Experimental Marine Biology and Ecology* 108:191-197.
- Reid, D. G. 1996. Systematics and evolution of *Littorina* / David G. Reid. London: Ray Society, 1996.
- Salo, P., E. Korpimäki, P. B. Banks, M. Nordström, and C. R. Dickman. 2007. Alien predators are more dangerous than native predators to prey populations. *Proceedings: Biological Sciences*:1237.
- Say, T. 1818. An account of the Crustacea of the United States. *Journal of the Academy of Natural Sciences of Philadelphia* 2:423.
- Scattergood, L. W. 1952. The distribution of the green crab, *Carcinides maenas* (L.) in the northwestern Atlantic. Fisheries Circular No. 8, Bulletin of the Department of Sea and Shore Fisheries, Augusta, Maine USA.

- Seeley, R. H. 1986. Intense natural selection caused a rapid morphological transition in a living marine snail. *Proceedings of the National Academy of Sciences of the United States of America*:6897.
- Smith, L. D. 2004. Biogeographic differences in claw size and performance in an introduced crab predator *Carcinus maenas*. *Marine Ecology Progress Series* 276:209-222.
- Smith, L. D., 2009. The role of phenotypic plasticity in marine biological invasions. Pages 177-202 in G. Rilov and J. A. Crooks, editors. *Biological invasions in marine ecosystems*. Springer e-books.
- Trussell, G. C. 1997. Phenotypic plasticity in the foot size of an intertidal snail. *Ecology*:1033.
- Trussell, G. C., and M. O. Nicklin. 2002. Cue sensitivity, inducible defense, and trade-offs in a marine snail. *Ecology*:1635.
- Trussell, G. C., and L. D. Smith. 2000. Induced defenses in response to an invading crab predator: an explanation of historical and geographic phenotypic change. *Proceedings of the National Academy of Sciences of the United States of America*:2123.
- Vitousek, P. M., H. A. Mooney, J. Lubchenco, and J. M. Melillo. 1997. Human domination of Earth's ecosystems. *Science* 277:494-499.
- Welch, W. R. and L. U. Churchill. Status of green crabs in Maine-1983. Research Reference Document 83/21. Maine Department of Marine Resources, Fisheries Research Lab, West Boothbay Harbor, Maine, USA.
- Werner, E. E., and G. G. Mittelbach. 1981. Optimal foraging: field tests of diet choice and habitat switching. *American Zoologist*:813.
- Yamada, S. B. 2001. Global invader: the European green crab / Sylvia Behrens Yamada. Corvallis, Or.: Oregon Sea Grant, Oregon State University; Seattle: Washington Sea Grant, c2001.